Axion DM Search with Vector Boson Fusion

A. Gurrola[1], **E. Sheridan**[1], B. Soubasis[1]

Vanderbilt University[1]

May 29, 2020

Table of Contents

Motivating Axions

Motivating Axions

Theoretical Origins

Motivating Axions

Theoretical Origins

- The structure of quantum chromodynamics permits a CP (charge conjugation-parity) symmetry violation, but experimental constraints require this violation to be small

Motivating Axions

Theoretical Origins

- The structure of quantum chromodynamics permits a CP (charge conjugation-parity) symmetry violation, but experimental constraints require this violation to be small
- It is unclear why this symmetry violation should simultaneously exist and be so small: this is the **strong CP problem**

Motivating Axions

Theoretical Origins

- The structure of quantum chromodynamics permits a CP (charge conjugation-parity) symmetry violation, but experimental constraints require this violation to be small
- It is unclear why this symmetry violation should simultaneously exist and be so small: this is the **strong CP problem**
- In 1977, Roberto Peccei and Helen Quinn addressed this conundrum by promoting the CP violation phase $\overline{\Theta}$—previously a Standard Model input requiring experimental measurement–to a scalar field which spontaneously breaks a new global symmetry (a Peccei–Quinn symmetry)

Motivating Axions

Theoretical Origins

- The structure of quantum chromodynamics permits a CP (charge conjugation-parity) symmetry violation, but experimental constraints require this violation to be small
- It is unclear why this symmetry violation should simultaneously exist and be so small: this is the **strong CP problem**
- In 1977, Roberto Peccei and Helen Quinn addressed this conundrum by promoting the CP violation phase $\overline{\Theta}$—previously a Standard Model input requiring experimental measurement–to a scalar field which spontaneously breaks a new global symmetry (a Peccei–Quinn symmetry)
- The quanta (or boson) of this new scalar field is the **axion**

Motivating Axions

Theoretical Origins

- The structure of quantum chromodynamics permits a CP (charge conjugation-parity) symmetry violation, but experimental constraints require this violation to be small
- It is unclear why this symmetry violation should simultaneously exist and be so small: this is the **strong CP problem**
- In 1977, Roberto Peccei and Helen Quinn addressed this conundrum by promoting the CP violation phase $\overline{\Theta}$—previously a Standard Model input requiring experimental measurement–to a scalar field which spontaneously breaks a new global symmetry (a Peccei–Quinn symmetry)
- The quanta (or boson) of this new scalar field is the **axion**

Axion Properties

Motivating Axions

Theoretical Origins

- The structure of quantum chromodynamics permits a CP (charge conjugation-parity) symmetry violation, but experimental constraints require this violation to be small
- It is unclear why this symmetry violation should simultaneously exist and be so small: this is the **strong CP problem**
- In 1977, Roberto Peccei and Helen Quinn addressed this conundrum by promoting the CP violation phase $\overline{\Theta}$—previously a Standard Model input requiring experimental measurement–to a scalar field which spontaneously breaks a new global symmetry (a Peccei–Quinn symmetry)
- The quanta (or boson) of this new scalar field is the **axion**

Axion Properties

- The axion is a **neutral spin-0 boson**, with different models permitting widely varied mass values

Motivating Axions

Theoretical Origins

- The structure of quantum chromodynamics permits a CP (charge conjugation-parity) symmetry violation, but experimental constraints require this violation to be small
- It is unclear why this symmetry violation should simultaneously exist and be so small: this is the **strong CP problem**
- In 1977, Roberto Peccei and Helen Quinn addressed this conundrum by promoting the CP violation phase $\overline{\Theta}$—previously a Standard Model input requiring experimental measurement–to a scalar field which spontaneously breaks a new global symmetry (a Peccei–Quinn symmetry)
- The quanta (or boson) of this new scalar field is the **axion**

Axion Properties

- The axion is a **neutral spin-0 boson**, with different models permitting widely varied mass values
- Light axions are compatible with current dark matter relic density calculations, making them dark matter candidates

Motivating Axions

Theoretical Origins

- The structure of quantum chromodynamics permits a CP (charge conjugation-parity) symmetry violation, but experimental constraints require this violation to be small
- It is unclear why this symmetry violation should simultaneously exist and be so small: this is the **strong CP problem**
- In 1977, Roberto Peccei and Helen Quinn addressed this conundrum by promoting the CP violation phase $\overline{\Theta}$—previously a Standard Model input requiring experimental measurement–to a scalar field which spontaneously breaks a new global symmetry (a Peccei–Quinn symmetry)
- The quanta (or boson) of this new scalar field is the **axion**

Axion Properties

- The axion is a **neutral spin-0 boson**, with different models permitting widely varied mass values
- Light axions are compatible with current dark matter relic density calculations, making them dark matter candidates
- Axion theories modify classical electrodynamics: in particular, the axion "rotates" the electric and magnetic fields into each other by an amount proportional to axion coupling and field strength

Motivating Axions

Theoretical Origins

- The structure of quantum chromodynamics permits a CP (charge conjugation-parity) symmetry violation, but experimental constraints require this violation to be small
- It is unclear why this symmetry violation should simultaneously exist and be so small: this is the **strong CP problem**
- In 1977, Roberto Peccei and Helen Quinn addressed this conundrum by promoting the CP violation phase $\overline{\Theta}$—previously a Standard Model input requiring experimental measurement–to a scalar field which spontaneously breaks a new global symmetry (a Peccei–Quinn symmetry)
- The quanta (or boson) of this new scalar field is the **axion**

Axion Properties

- The axion is a **neutral spin-0 boson**, with different models permitting widely varied mass values
- Light axions are compatible with current dark matter relic density calculations, making them dark matter candidates
- Axion theories modify classical electrodynamics: in particular, the axion "rotates" the electric and magnetic fields into each other by an amount proportional to axion coupling and field strength

Axion Literature

Motivating Axions

Theoretical Origins

- The structure of quantum chromodynamics permits a CP (charge conjugation-parity) symmetry violation, but experimental constraints require this violation to be small
- It is unclear why this symmetry violation should simultaneously exist and be so small: this is the **strong CP problem**
- In 1977, Roberto Peccei and Helen Quinn addressed this conundrum by promoting the CP violation phase $\overline{\Theta}$—previously a Standard Model input requiring experimental measurement–to a scalar field which spontaneously breaks a new global symmetry (a Peccei–Quinn symmetry)
- The quanta (or boson) of this new scalar field is the **axion**

Axion Properties

- The axion is a **neutral spin-0 boson**, with different models permitting widely varied mass values
- Light axions are compatible with current dark matter relic density calculations, making them dark matter candidates
- Axion theories modify classical electrodynamics: in particular, the axion "rotates" the electric and magnetic fields into each other by an amount proportional to axion coupling and field strength

Axion Literature

- Astrophysics/cosmological experiments investigate axions and axion-like particles (ALPs) with eV scale masses, placing upper bounds on those masses (given certain assumptions on couplings)

Motivating Axions

Theoretical Origins

- The structure of quantum chromodynamics permits a CP (charge conjugation-parity) symmetry violation, but experimental constraints require this violation to be small
- It is unclear why this symmetry violation should simultaneously exist and be so small: this is the **strong CP problem**
- In 1977, Roberto Peccei and Helen Quinn addressed this conundrum by promoting the CP violation phase $\overline{\Theta}$—previously a Standard Model input requiring experimental measurement–to a scalar field which spontaneously breaks a new global symmetry (a Peccei–Quinn symmetry)
- The quanta (or boson) of this new scalar field is the **axion**

Axion Properties

- The axion is a **neutral spin-0 boson**, with different models permitting widely varied mass values
- Light axions are compatible with current dark matter relic density calculations, making them dark matter candidates
- Axion theories modify classical electrodynamics: in particular, the axion "rotates" the electric and magnetic fields into each other by an amount proportional to axion coupling and field strength

Axion Literature

- Astrophysics/cosmological experiments investigate axions and axion-like particles (ALPs) with eV scale masses, placing upper bounds on those masses (given certain assumptions on couplings)
- However, there still exist models which enable heavy axions and ALPs to have masses in the MeV and GeV scales, which have been studied at the LHC (primarily at the 100s of GeV scale, due to sensitivity limitations)

Motivating Axions

Theoretical Origins

- The structure of quantum chromodynamics permits a CP (charge conjugation-parity) symmetry violation, but experimental constraints require this violation to be small
- It is unclear why this symmetry violation should simultaneously exist and be so small: this is the **strong CP problem**
- In 1977, Roberto Peccei and Helen Quinn addressed this conundrum by promoting the CP violation phase $\overline{\Theta}$—previously a Standard Model input requiring experimental measurement–to a scalar field which spontaneously breaks a new global symmetry (a Peccei–Quinn symmetry)
- The quanta (or boson) of this new scalar field is the **axion**

Axion Properties

- The axion is a **neutral spin-0 boson**, with different models permitting widely varied mass values
- Light axions are compatible with current dark matter relic density calculations, making them dark matter candidates
- Axion theories modify classical electrodynamics: in particular, the axion "rotates" the electric and magnetic fields into each other by an amount proportional to axion coupling and field strength

Axion Literature

- Astrophysics/cosmological experiments investigate axions and axion-like particles (ALPs) with eV scale masses, placing upper bounds on those masses (given certain assumptions on couplings)
- However, there still exist models which enable heavy axions and ALPs to have masses in the MeV and GeV scales, which have been studied at the LHC (primarily at the 100s of GeV scale, due to sensitivity limitations)
- An unexplored gap exists between the probed axion masses at non-collider and at collider experiments (the MeV scale), motivating the focus our phenomenology project

Motivating the Vector Boson Fusion Approach

Motivating the Vector Boson Fusion Approach

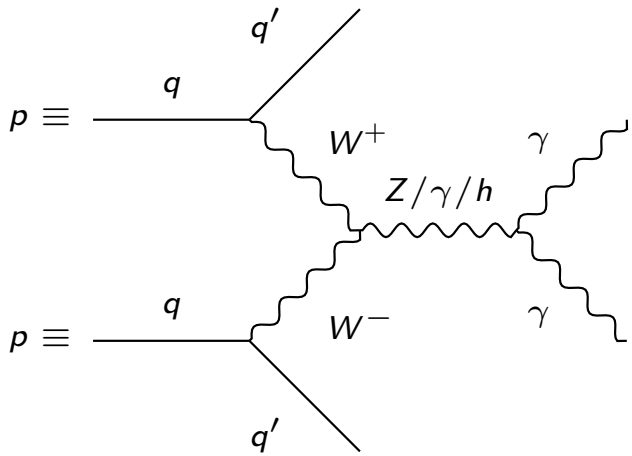

Motivating the Vector Boson Fusion Approach

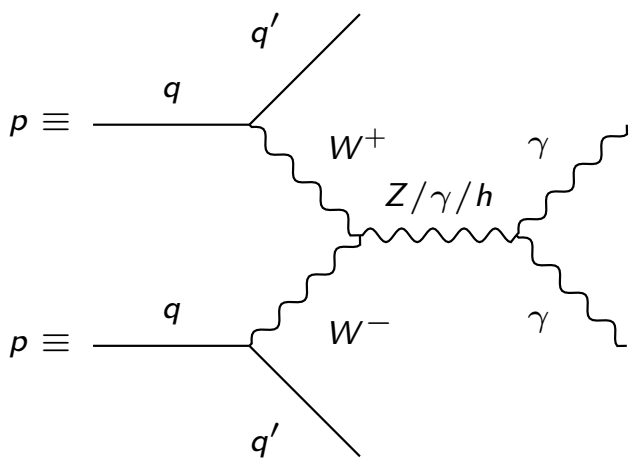

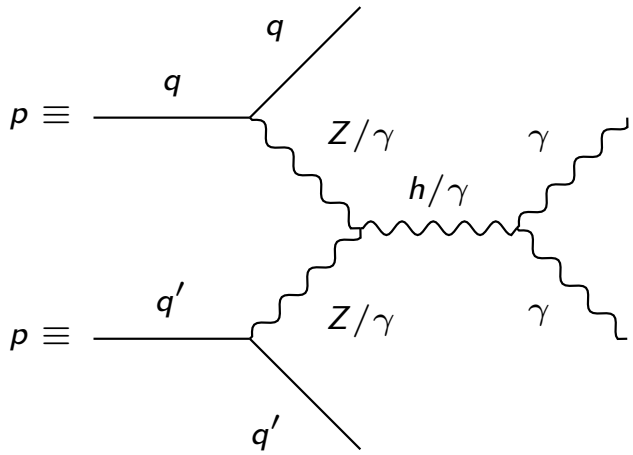

Motivating the Vector Boson Fusion Approach

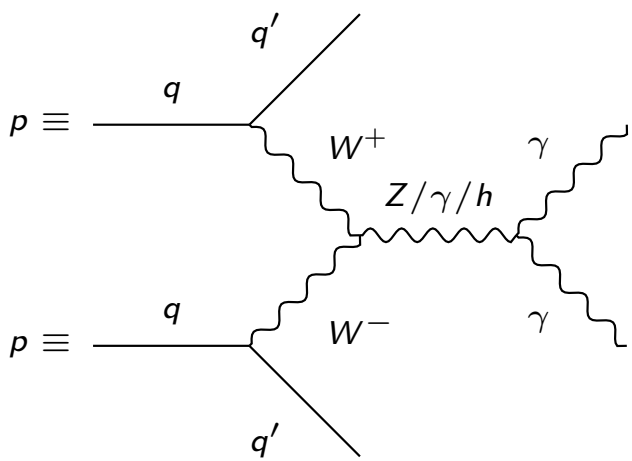

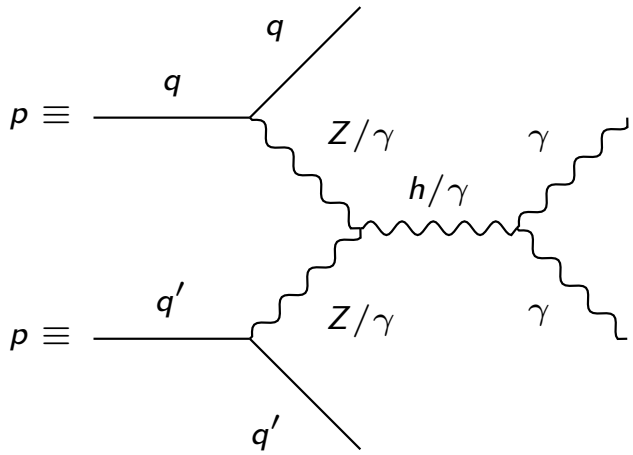

Description

Motivating the Vector Boson Fusion Approach

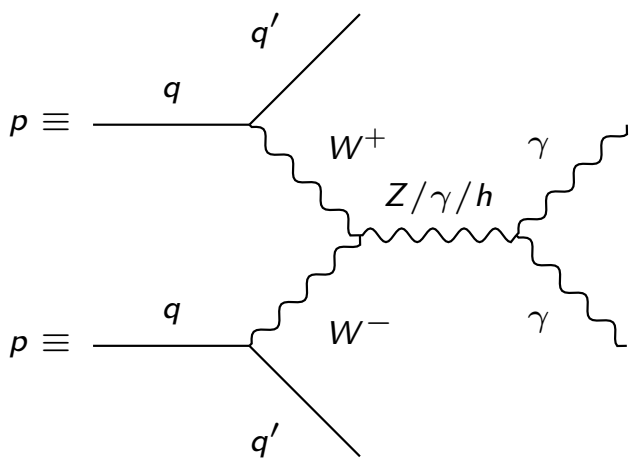

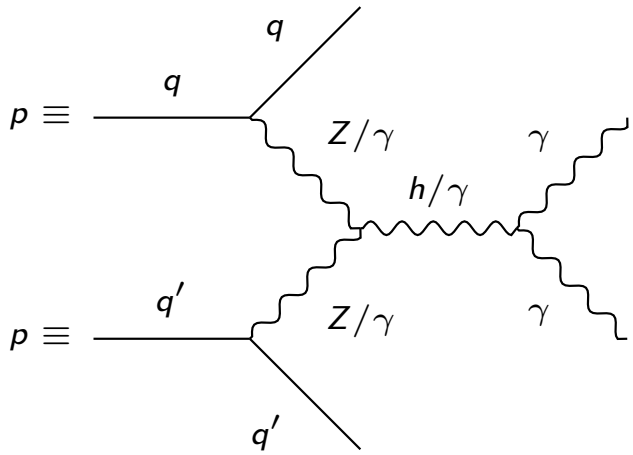

Description

- Vector boson fusion processes (VBF) are experimentally important due to their distinctiveness at the LHC (prototypical Feynman diagram given above)

Motivating the Vector Boson Fusion Approach

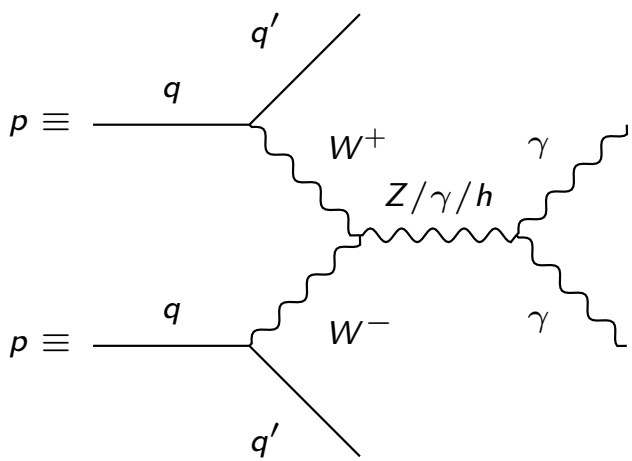

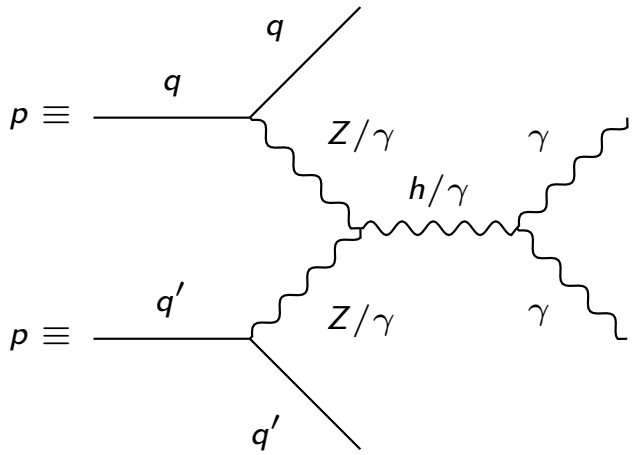

Description

- Vector boson fusion processes (VBF) are experimentally important due to their distinctiveness at the LHC (prototypical Feynman diagram given above)
    - In particular, the "tagged jets" (produced by the outgoing quarks) carry a high difference between their **pseudorapidities**

Motivating the Vector Boson Fusion Approach

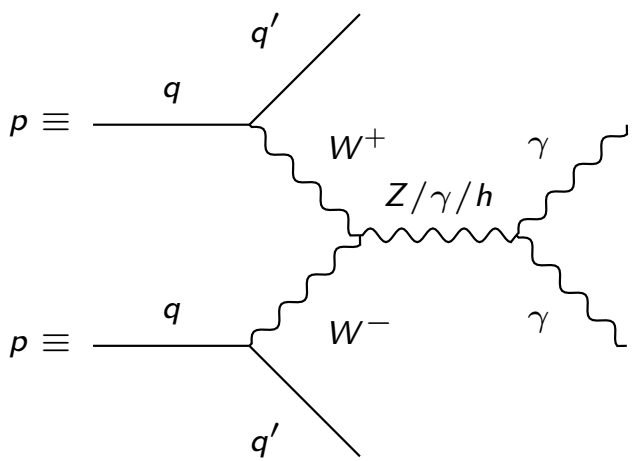

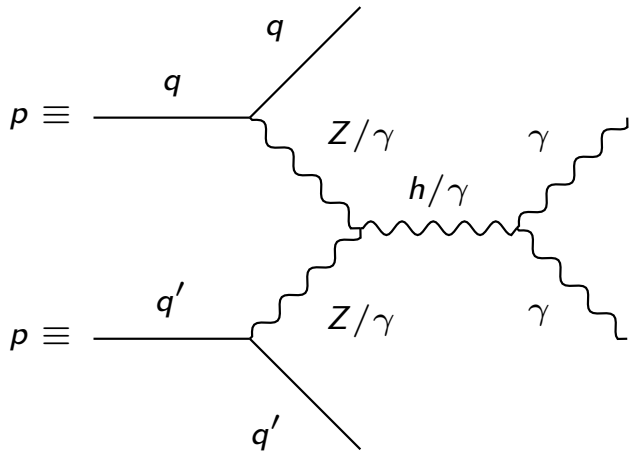

Description

- Vector boson fusion processes (VBF) are experimentally important due to their distinctiveness at the LHC (prototypical Feynman diagram given above)
  - In particular, the "tagged jets" (produced by the outgoing quarks) carry a high difference between their **pseudorapidities**
  - This VBF kinematic signature suppresses many background channels, including those both with and without QCD vertices

Motivating the Vector Boson Fusion Approach

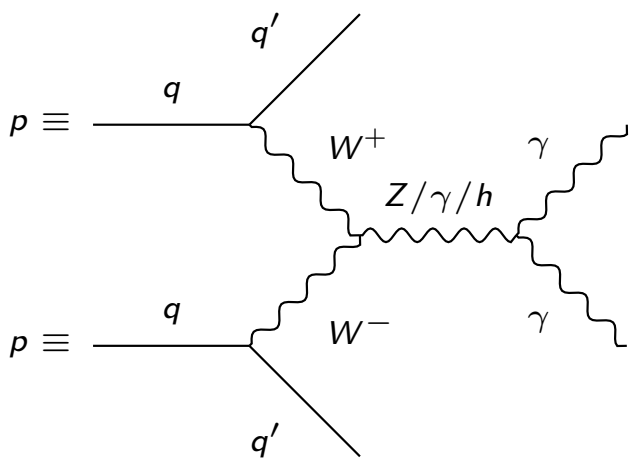

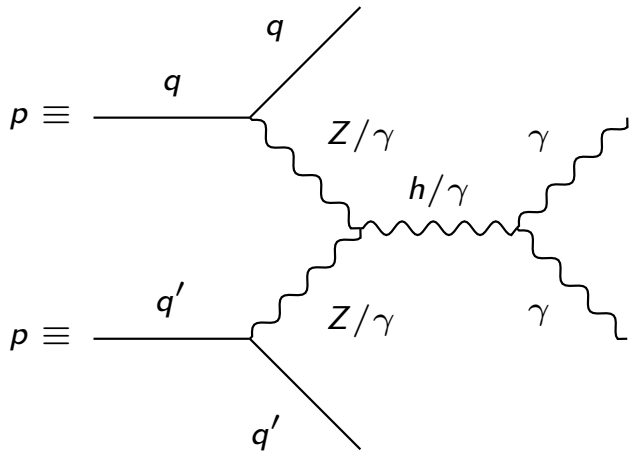

Description

- Vector boson fusion processes (VBF) are experimentally important due to their distinctiveness at the LHC (prototypical Feynman diagram given above)
  - In particular, the "tagged jets" (produced by the outgoing quarks) carry a high difference between their **pseudorapidities**
  - This VBF kinematic signature suppresses many background channels, including those both with and without QCD vertices
- VBF cross sections typically surpass those of other topologies (Drell-Yan, etc) in new-physics processes with sufficiently heavy new particles (at around the TeV scale)

Signal Generation

Signal Generation

Process

Signal Generation

Process

- Signal generated using **MadGraph** (version **2.6.5**) with the following command

```
import model ALP_chiral_UFO
generate p p > ax j j QCD=0, ax > a a
```

Signal Generation

Process

- Signal generated using **MadGraph** (version **2.6.5**) with the following command

```
import model ALP_chiral_UFO
generate p p > ax j j QCD=0, ax > a a
```

- Our studies focus on an axion mass of **1 MeV**

Signal Generation

Process

- Signal generated using **MadGraph** (version **2.6.5**) with the following command

```
import model ALP_chiral_UFO
generate p p > ax j j QCD=0, ax > a a
```

- Our studies focus on an axion mass of **1 MeV**
- Only default MadGraph cuts employed: e.g., $p_T^j > 20$ GeV, $p_T^\gamma > 10$ GeV

Signal Generation

Process

- Signal generated using **MadGraph** (version **2.6.5**) with the following command

```
import model ALP_chiral_UFO
generate p p > ax j j QCD=0, ax > a a
```

- Our studies focus on an axion mass of **1 MeV**
- Only default MadGraph cuts employed: e.g., $p_T^j > 20$ GeV, $p_T^\gamma > 10$ GeV

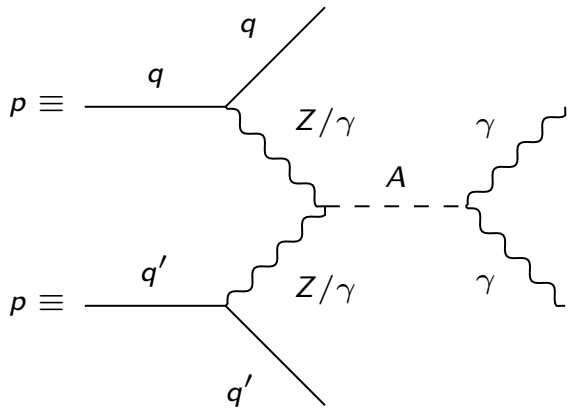

Signal Generation

Process

- Signal generated using **MadGraph** (version **2.6.5**) with the following command

```
import model ALP_chiral_UFO
generate p p > ax j j QCD=0, ax > a a
```

- Our studies focus on an axion mass of **1 MeV**
- Only default MadGraph cuts employed: e.g., $p_T^j > 20$ GeV, $p_T^\gamma > 10$ GeV

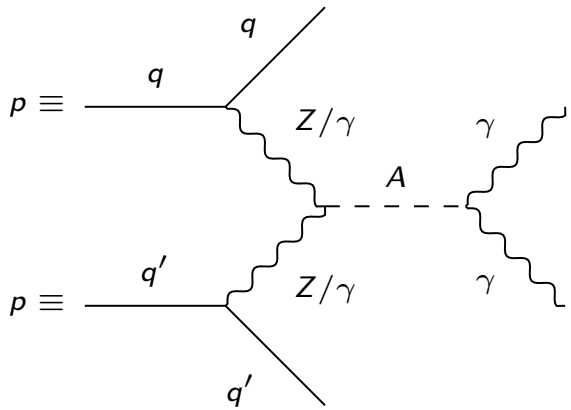

Comments

Signal Generation

Process

- Signal generated using **MadGraph** (version **2.6.5**) with the following command

```
import model ALP_chiral_UFO
generate p p > ax j j QCD=0, ax > a a
```

- Our studies focus on an axion mass of **1 MeV**
- Only default MadGraph cuts employed: e.g., $p_T^j > 20$ GeV, $p_T^\gamma > 10$ GeV

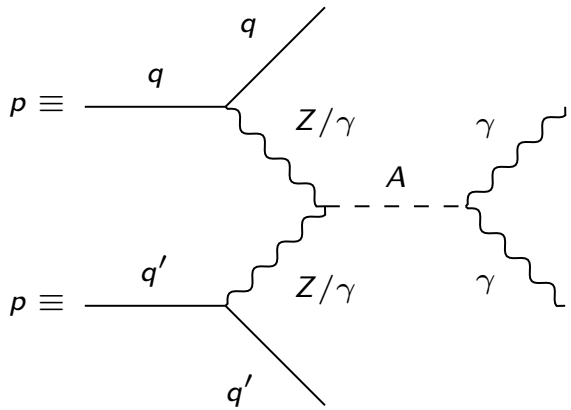

Comments

- `QCD = 0` selected due to our interest in axions with **negligible strong force couplings**

Signal Generation

Process

- Signal generated using **MadGraph** (version **2.6.5**) with the following command

```
import model ALP_chiral_UFO
generate p p > ax j j QCD=0, ax > a a
```

- Our studies focus on an axion mass of **1 MeV**
- Only default MadGraph cuts employed: e.g., $p_T^j > 20$ GeV, $p_T^\gamma > 10$ GeV

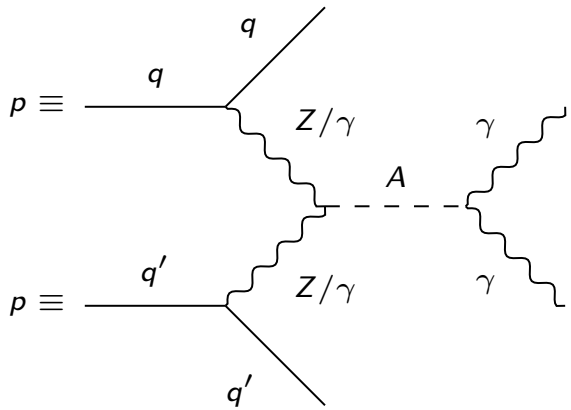

Comments

- `QCD = 0` selected due to our interest in axions with **negligible strong force couplings**
- `ax > a a` channel selected due to our emphasis on **lighter axions** (photons dominating heavier bosons)

Signal Generation

Process

- Signal generated using **MadGraph** (version **2.6.5**) with the following command

```
import model ALP_chiral_UFO
generate p p > ax j j QCD=0, ax > a a
```

- Our studies focus on an axion mass of **1 MeV**
- Only default MadGraph cuts employed: e.g., $p_T^j > 20$ GeV, $p_T^\gamma > 10$ GeV

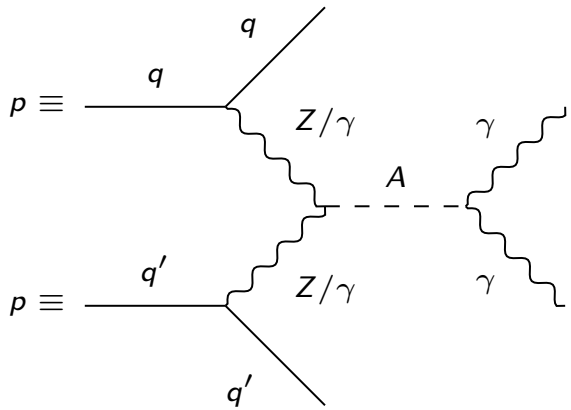

Comments

- `QCD = 0` selected due to our interest in axions with **negligible strong force couplings**
- `ax > a a` channel selected due to our emphasis on **lighter axions** (photons dominating heavier bosons)
- The significance of our studies arises in part from small axion mass scales probed

Initial Kinematics

Initial Kinematics

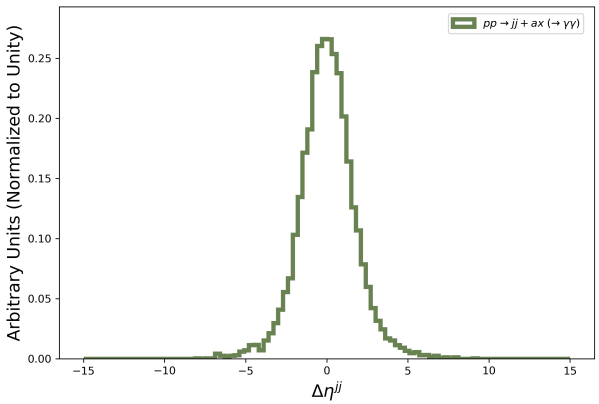

Initial Kinematics

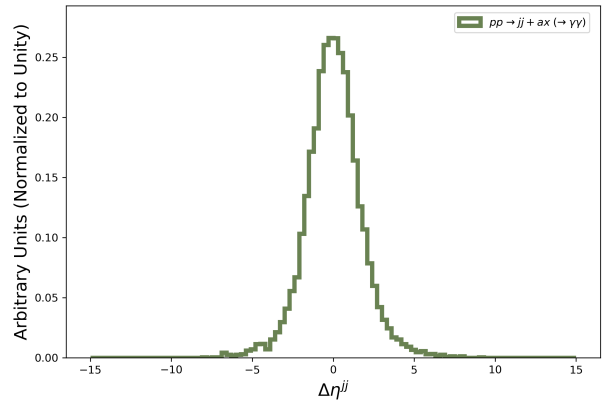

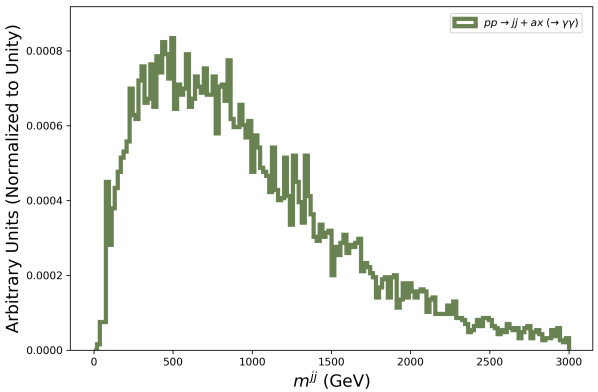

Initial Kinematics

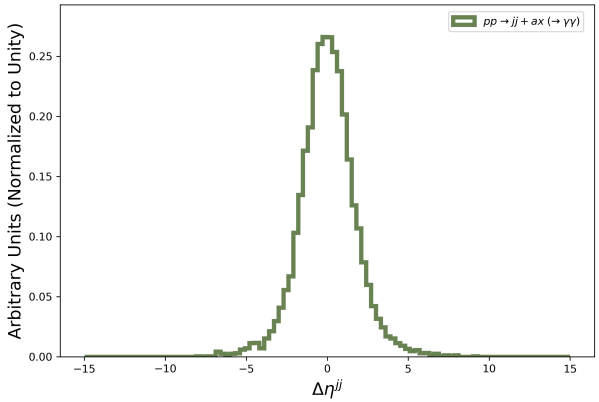

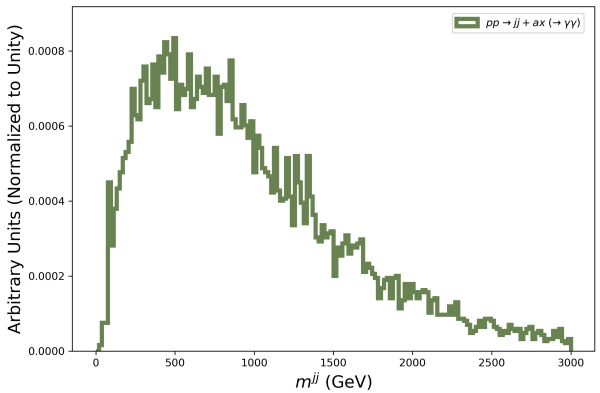

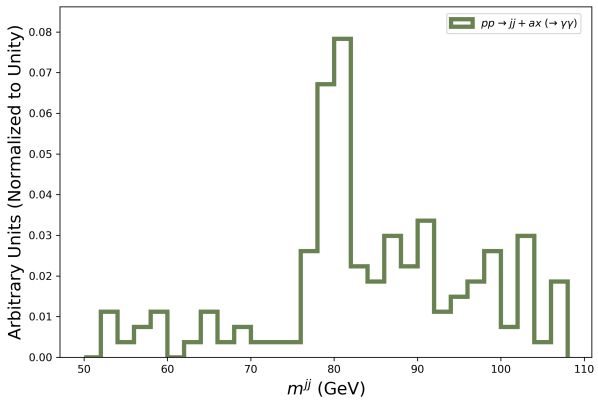

Initial Kinematics

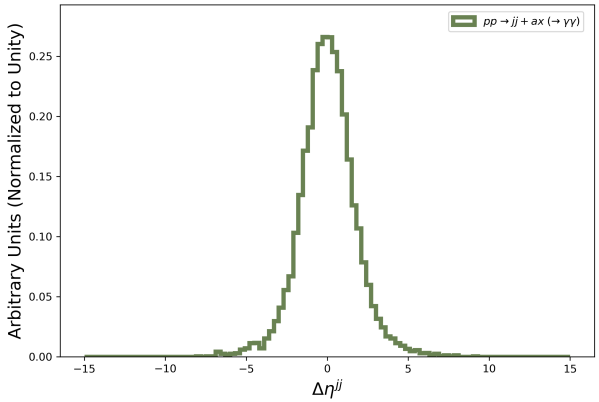

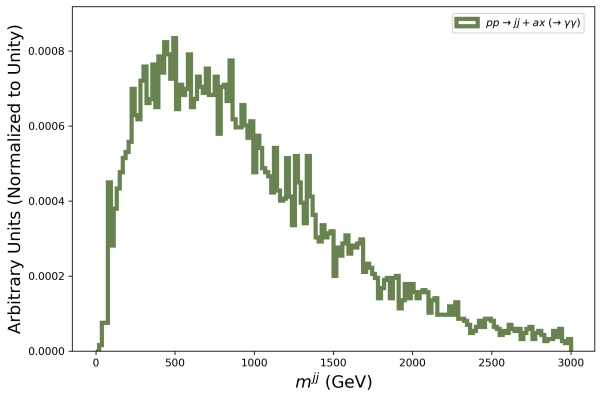

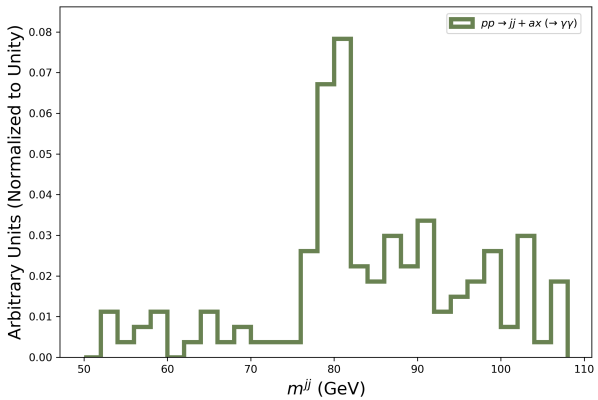

Comments

Initial Kinematics

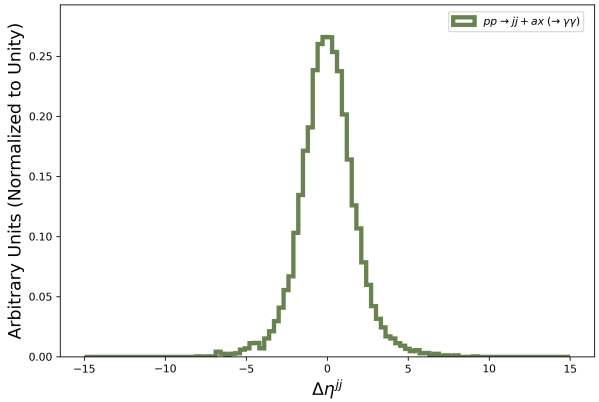

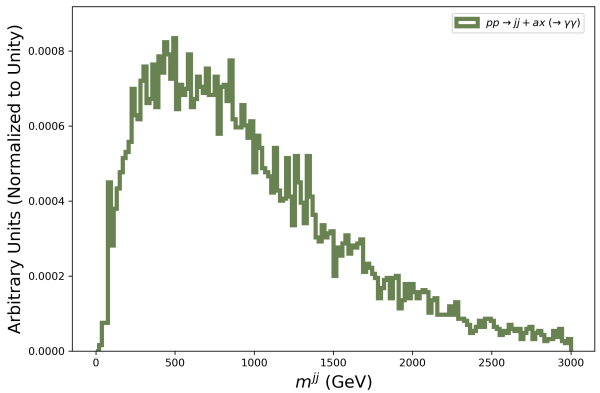

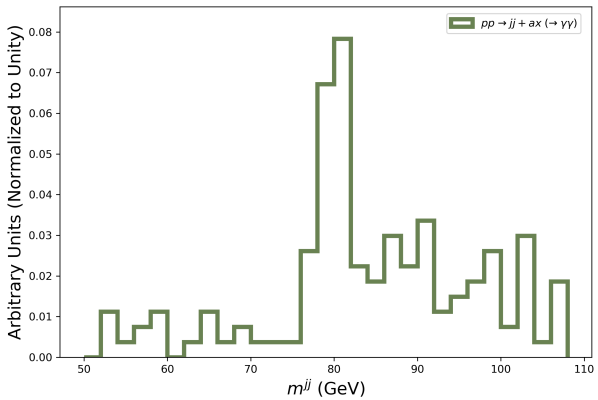

Comments

- VBF processes are characterized by high $|\Delta\eta^{jj}|$: a peak at 0 indicates the dominance of other processes

Initial Kinematics

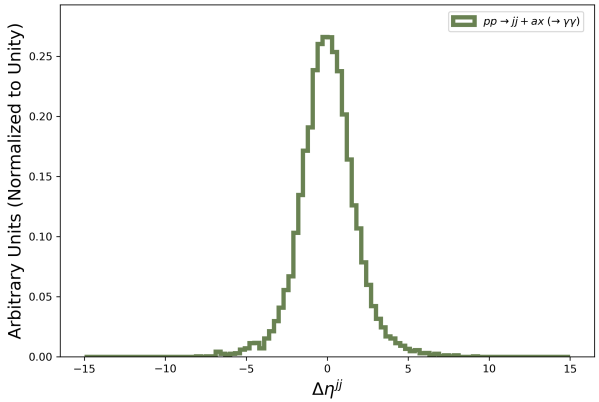

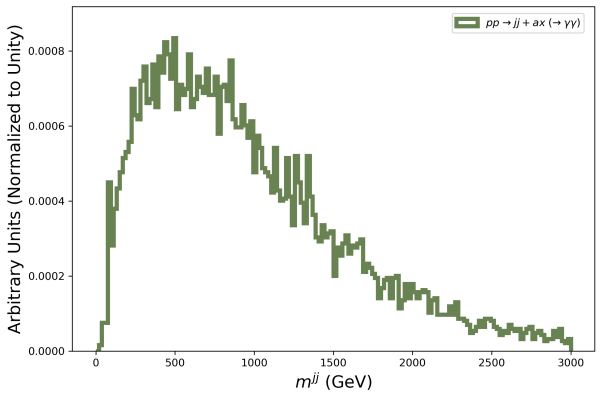

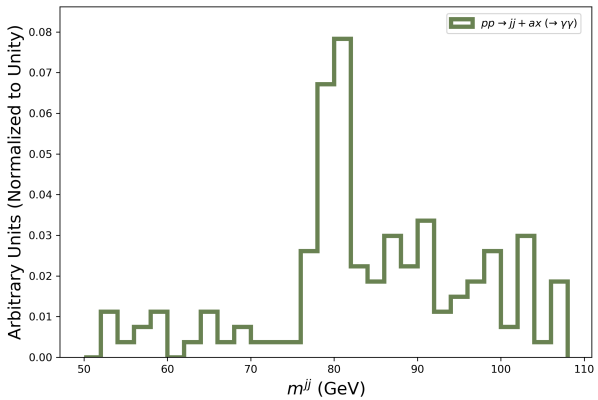

Comments

- VBF processes are characterized by high $|\Delta\eta^{jj}|$: a peak at 0 indicates the dominance of other processes
- The m^{jj} peak at approx. 80-90 GeV points to contributions from `Z/W+/W- > j j` processes (associated axion production)

Initial Kinematics

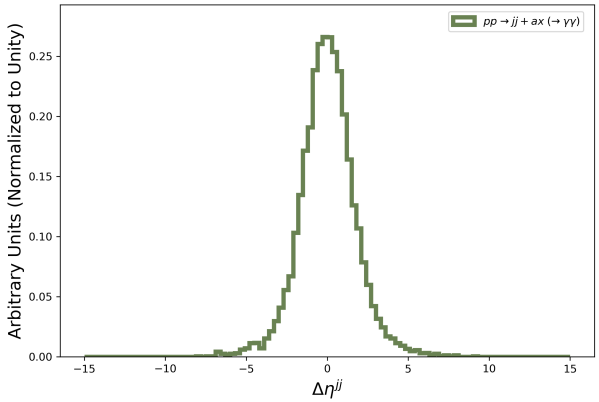

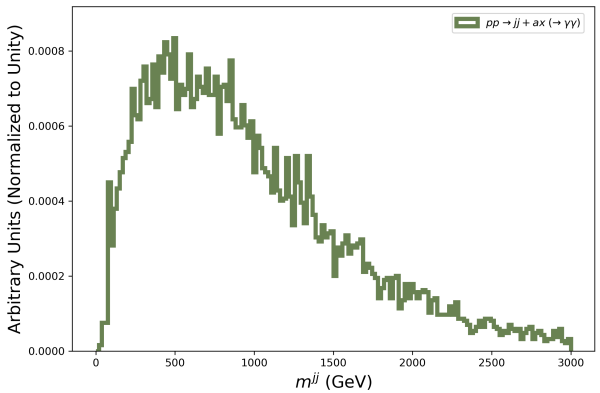

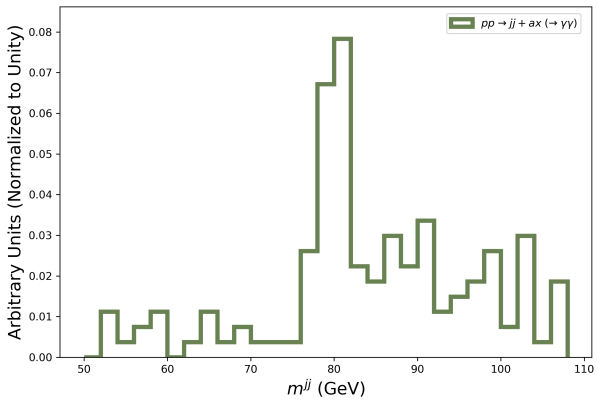

Comments

- VBF processes are characterized by high $|\Delta\eta^{jj}|$: a peak at 0 indicates the dominance of other processes
- The m^{jj} peak at approx. 80-90 GeV points to contributions from `Z/W+/W- > j j` processes (associated axion production)
- Total cross section for signal is 0.786 ± 0.001 pb

Channel	Cross-Section (pb)
`g g > ax g g`	$0.731 \pm$ 1e-3
`u d > ax u d`	$0.02414 \pm$ 2e-4
`u u > ax u u`	$0.01549 \pm$ 6e-5

Initial Kinematics

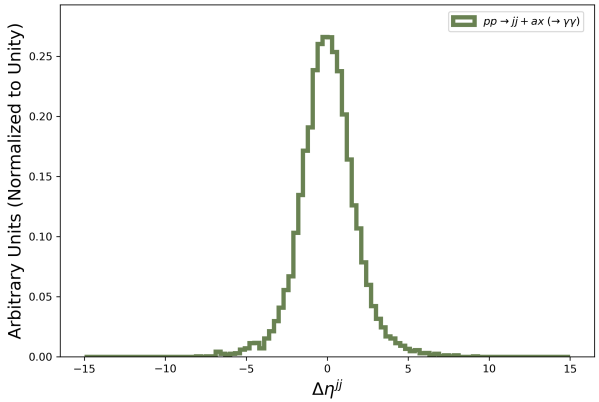

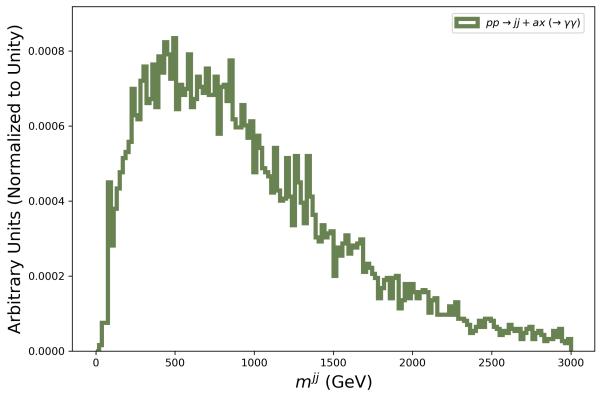

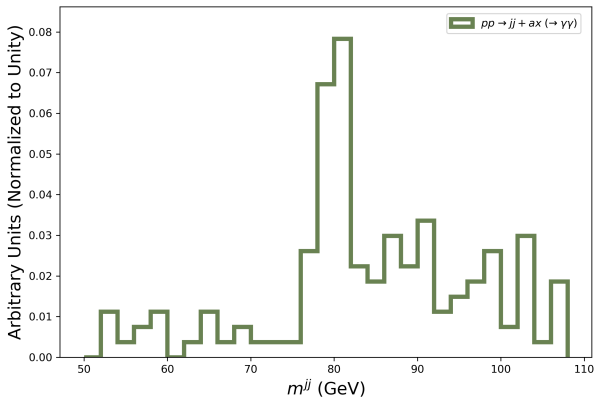

Comments

- VBF processes are characterized by high $|\Delta\eta^{jj}|$: a peak at 0 indicates the dominance of other processes
- The m^{jj} peak at approx. 80-90 GeV points to contributions from `Z/W+/W- > j j` processes (associated axion production)
- Total cross section for signal is 0.786 ± 0.001 pb

Channel	Cross-Section (pb)
`g g > ax g g`	$0.731 \pm$ 1e-3
`u d > ax u d`	$0.02414 \pm$ 2e-4
`u u > ax u u`	$0.01549 \pm$ 6e-5

- Channel with next highest cross section on order of 1 fb.

Initial Kinematics

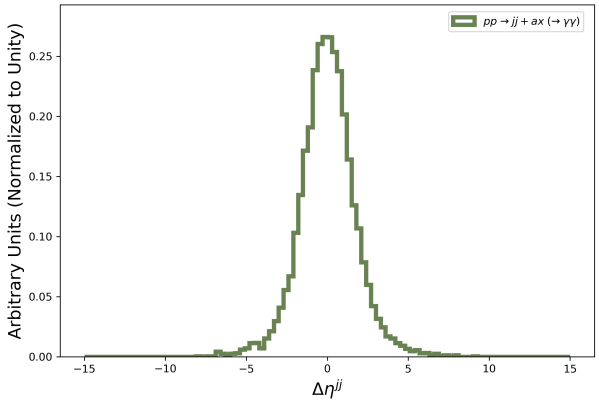

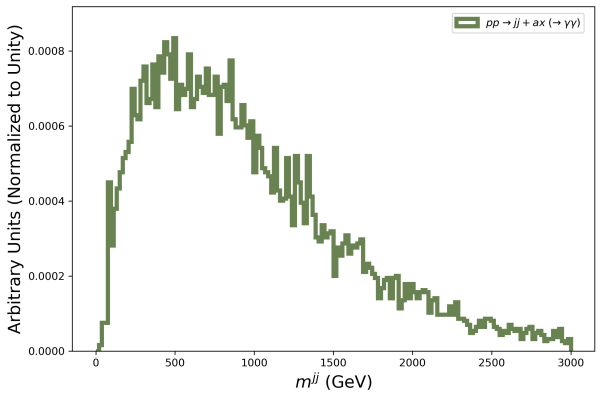

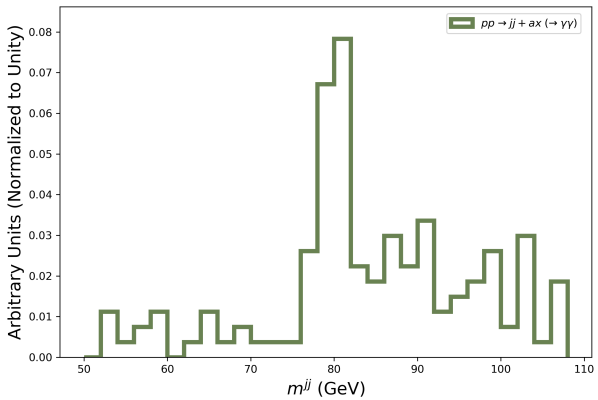

Comments

- VBF processes are characterized by high $|\Delta\eta^{jj}|$: a peak at 0 indicates the dominance of other processes
- The m^{jj} peak at approx. 80-90 GeV points to contributions from `Z/W+/W- > j j` processes (associated axion production)
- Total cross section for signal is 0.786 ± 0.001 pb

Channel	Cross-Section (pb)
`g g > ax g g`	$0.731 \pm$ 1e-3
`u d > ax u d`	$0.02414 \pm$ 2e-4
`u u > ax u u`	$0.01549 \pm$ 6e-5

- Channel with next highest cross section on order of 1 fb.
- `q q > ax q q` processes can take on a VBF topology, but the `g g > ax g g` channel does not

Initial Kinematics

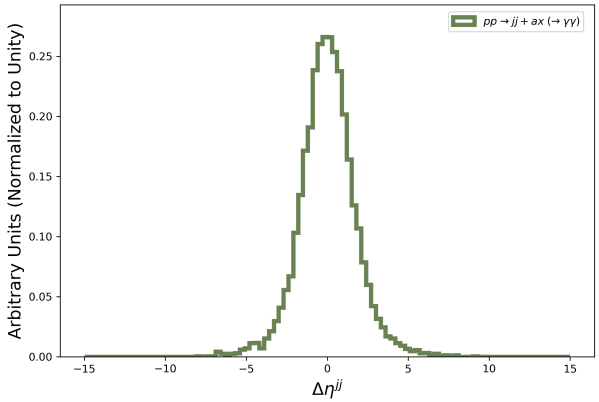

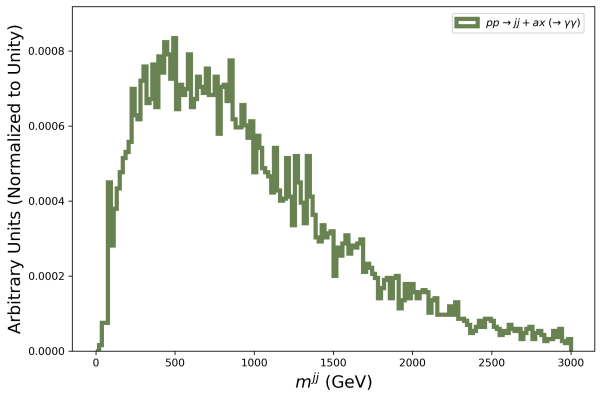

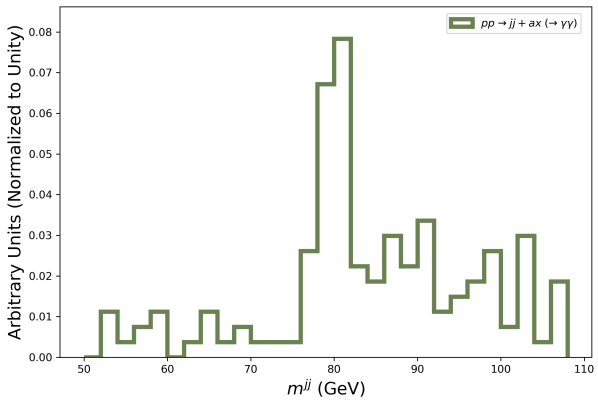

Comments

- VBF processes are characterized by high $|\Delta\eta^{jj}|$: a peak at 0 indicates the dominance of other processes
- The m^{jj} peak at approx. 80-90 GeV points to contributions from `Z/W+/W- > j j` processes (associated axion production)
- Total cross section for signal is 0.786 ± 0.001 pb

Channel	Cross-Section (pb)
`g g > ax g g`	$0.731 \pm$ 1e-3
`u d > ax u d`	$0.02414 \pm$ 2e-4
`u u > ax u u`	$0.01549 \pm$ 6e-5

- Channel with next highest cross section on order of 1 fb.
- `q q > ax q q` processes can take on a VBF topology, but the `g g > ax g g` channel does not
- Despite the higher cross section, we avoid gluon-gluon processes for several reasons

Initial Kinematics

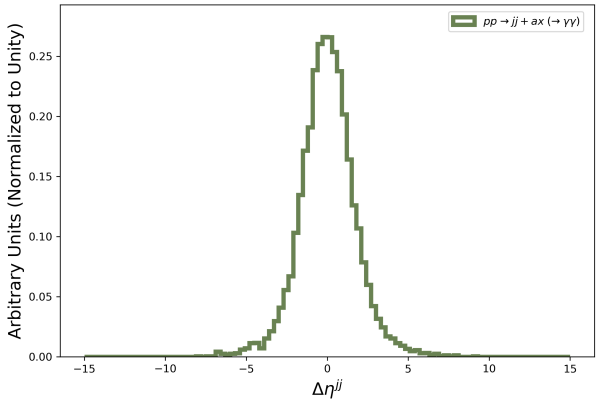

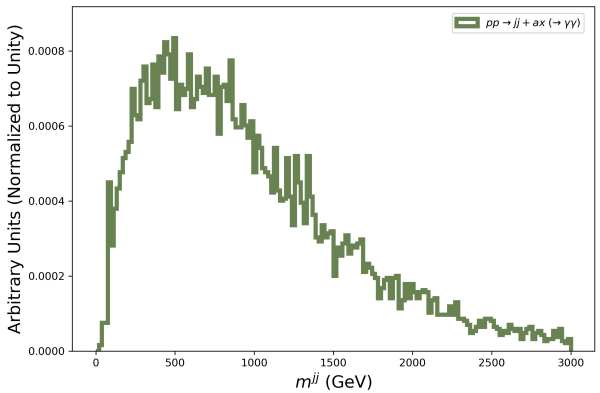

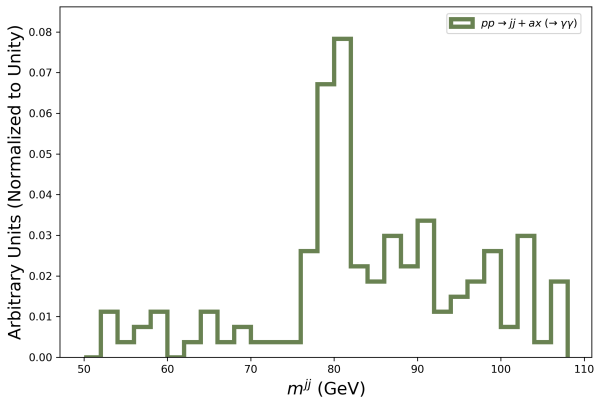

Comments

- VBF processes are characterized by high $|\Delta\eta^{jj}|$: a peak at 0 indicates the dominance of other processes
- The m^{jj} peak at approx. 80-90 GeV points to contributions from `Z/W+/W- > j j` processes (associated axion production)
- Total cross section for signal is 0.786 ± 0.001 pb

Channel	Cross-Section (pb)
`g g > ax g g`	$0.731 \pm$ 1e-3
`u d > ax u d`	$0.02414 \pm$ 2e-4
`u u > ax u u`	$0.01549 \pm$ 6e-5

- Channel with next highest cross section on order of 1 fb.
- `q q > ax q q` processes can take on a VBF topology, but the `g g > ax g g` channel does not
- Despite the higher cross section, we avoid gluon-gluon processes for several reasons
  - Predominately low $|\Delta\eta^{jj}|$ (lower discriminating power)

Initial Kinematics

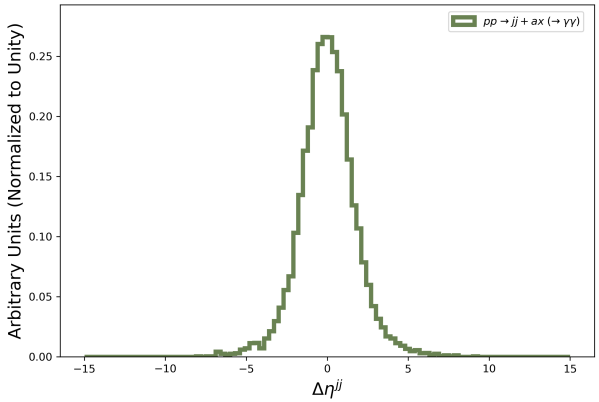

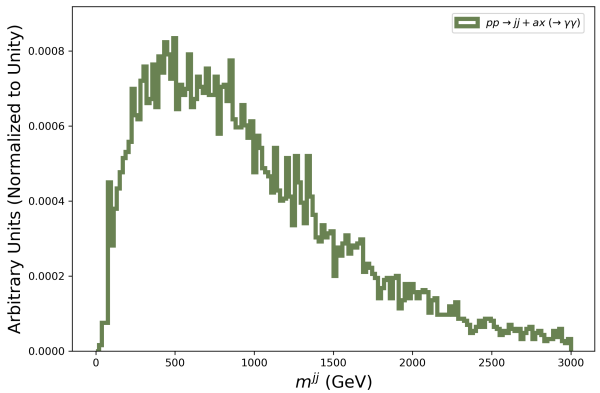

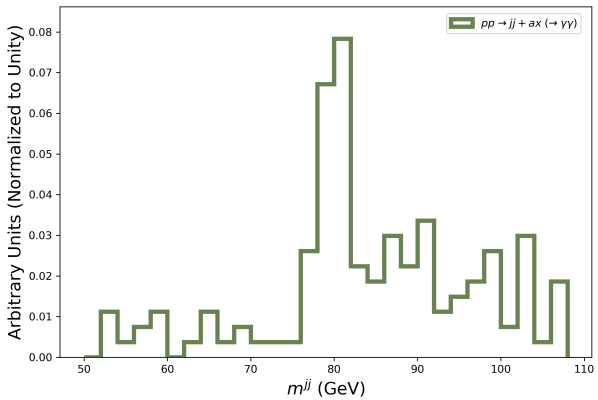

Comments

- VBF processes are characterized by high $|\Delta\eta^{jj}|$: a peak at 0 indicates the dominance of other processes
- The m^{jj} peak at approx. 80-90 GeV points to contributions from `Z/W+/W- > j j` processes (associated axion production)
- Total cross section for signal is 0.786 ± 0.001 pb

Channel	Cross-Section (pb)
`g g > ax g g`	$0.731 \pm$ 1e-3
`u d > ax u d`	$0.02414 \pm$ 2e-4
`u u > ax u u`	$0.01549 \pm$ 6e-5

- Channel with next highest cross section on order of 1 fb.
- `q q > ax q q` processes can take on a VBF topology, but the `g g > ax g g` channel does not
- Despite the higher cross section, we avoid gluon-gluon processes for several reasons
  - Predominately low $|\Delta\eta^{jj}|$ (lower discriminating power)
  - Extensively studied in previous axion research

Initial Kinematics

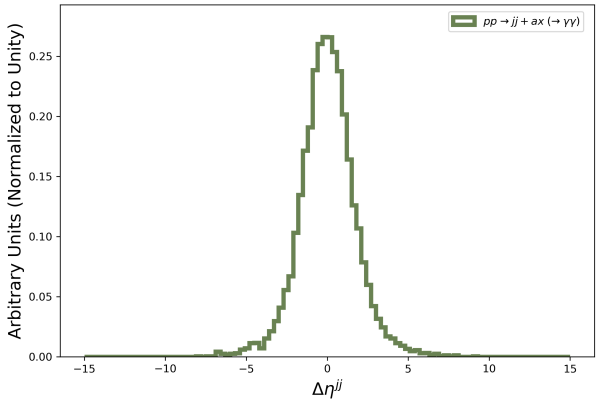

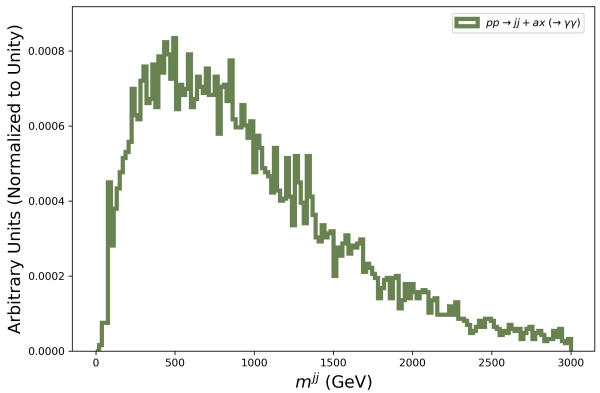

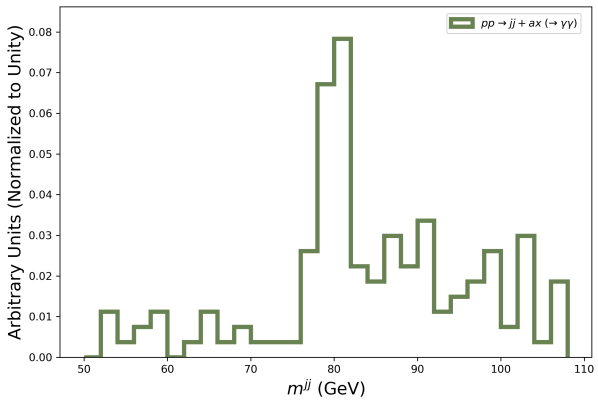

Comments

- VBF processes are characterized by high $|\Delta\eta^{jj}|$: a peak at 0 indicates the dominance of other processes
- The m^{jj} peak at approx. 80-90 GeV points to contributions from `Z/W+/W- > j j` processes (associated axion production)
- Total cross section for signal is 0.786 ± 0.001 pb

Channel	Cross-Section (pb)
`g g > ax g g`	$0.731 \pm$ 1e-3
`u d > ax u d`	$0.02414 \pm$ 2e-4
`u u > ax u u`	$0.01549 \pm$ 6e-5

- Channel with next highest cross section on order of 1 fb.
- `q q > ax q q` processes can take on a VBF topology, but the `g g > ax g g` channel does not
- Despite the higher cross section, we avoid gluon-gluon processes for several reasons
  - Predominately low $|\Delta\eta^{jj}|$ (lower discriminating power)
  - Extensively studied in previous axion research
  - Shown to be largely insensitive to light axions

Increasing VBF Purity in Signal

Increasing VBF Purity in Signal

Objective

Increasing VBF Purity in Signal

Objective

- Want to generate signal events in a phase space region which emphasizes our eventual optimization (ensuring sufficient statistics)

Increasing VBF Purity in Signal

Objective

- Want to generate signal events in a phase space region which emphasizes our eventual optimization (ensuring sufficient statistics)
- Equivalently, want to generate signal events with the particular topologies (VBF) we will later select

Increasing VBF Purity in Signal

Objective

- Want to generate signal events in a phase space region which emphasizes our eventual optimization (ensuring sufficient statistics)
- Equivalently, want to generate signal events with the particular topologies (VBF) we will later select
- Thus before comparing with background, want to impose **MadGraph-level cuts** on signal events

Increasing VBF Purity in Signal

Objective

- Want to generate signal events in a phase space region which emphasizes our eventual optimization (ensuring sufficient statistics)
- Equivalently, want to generate signal events with the particular topologies (VBF) we will later select
- Thus before comparing with background, want to impose **MadGraph-level cuts** on signal events
- Two topologies being targeted by our cuts: `g g > ax g g` and `Z/W > j j`

Increasing VBF Purity in Signal

Objective

- Want to generate signal events in a phase space region which emphasizes our eventual optimization (ensuring sufficient statistics)
- Equivalently, want to generate signal events with the particular topologies (VBF) we will later select
- Thus before comparing with background, want to impose **MadGraph-level cuts** on signal events
- Two topologies being targeted by our cuts: `g g > ax g g` and `Z/W > j j`

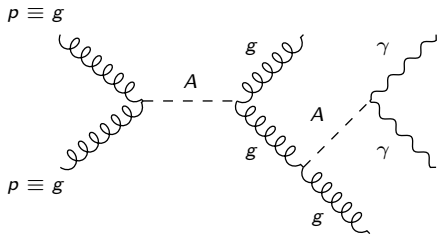

Increasing VBF Purity in Signal

Objective

- Want to generate signal events in a phase space region which emphasizes our eventual optimization (ensuring sufficient statistics)
- Equivalently, want to generate signal events with the particular topologies (VBF) we will later select
- Thus before comparing with background, want to impose **MadGraph-level cuts** on signal events
- Two topologies being targeted by our cuts: `g g > ax g g` and `Z/W > j j`

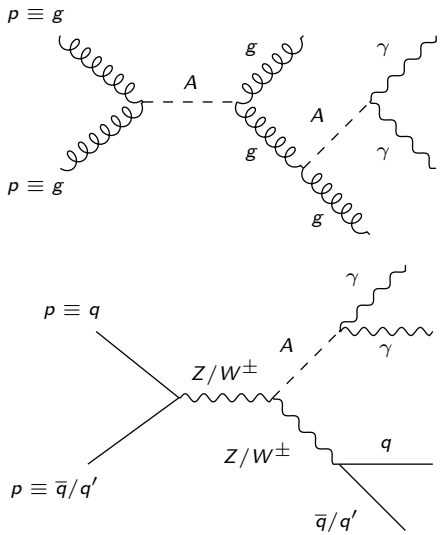

Increasing VBF Purity in Signal

Objective

- Want to generate signal events in a phase space region which emphasizes our eventual optimization (ensuring sufficient statistics)
- Equivalently, want to generate signal events with the particular topologies (VBF) we will later select
- Thus before comparing with background, want to impose **MadGraph-level cuts** on signal events
- Two topologies being targeted by our cuts: `g g > ax g g` and `Z/W > j j`

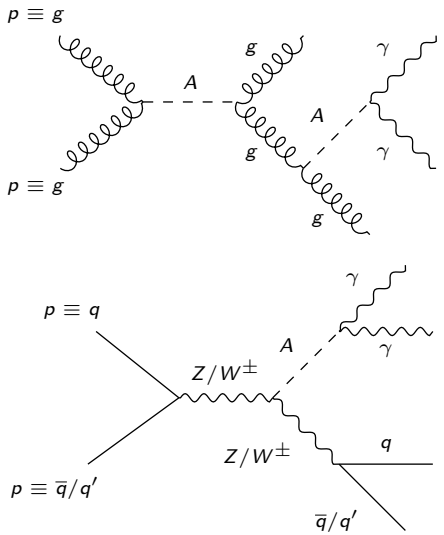

Final Approach

Increasing VBF Purity in Signal

Objective

- Want to generate signal events in a phase space region which emphasizes our eventual optimization (ensuring sufficient statistics)
- Equivalently, want to generate signal events with the particular topologies (VBF) we will later select
- Thus before comparing with background, want to impose **MadGraph-level cuts** on signal events
- Two topologies being targeted by our cuts: `g g > ax g g` and `Z/W > j j`

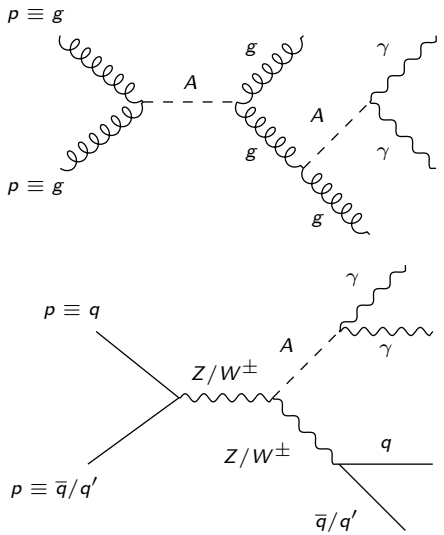

Final Approach

- Choose to generate 1000000 signal events with all of the previous commands/setting, along with the following additional MadGraph selections.

  $|\Delta\eta^{jj}| > 2.4$, $m^{jj} > 120$ GeV

Increasing VBF Purity in Signal

Objective

- Want to generate signal events in a phase space region which emphasizes our eventual optimization (ensuring sufficient statistics)
- Equivalently, want to generate signal events with the particular topologies (VBF) we will later select
- Thus before comparing with background, want to impose **MadGraph-level cuts** on signal events
- Two topologies being targeted by our cuts: `g g > ax g g` and `Z/W > j j`

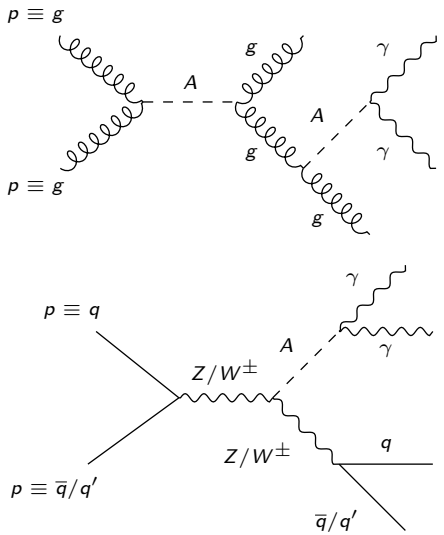

Final Approach

- Choose to generate 1000000 signal events with all of the previous commands/setting, along with the following additional MadGraph selections.

  $|\Delta\eta^{jj}| > 2.4$, $m^{jj} > 120$ GeV

  - The gluon-gluon channel primarily exhibits low $|\Delta\eta^{jj}|$, so we apply a cut there to reduce its cross section

Increasing VBF Purity in Signal

Objective

- Want to generate signal events in a phase space region which emphasizes our eventual optimization (ensuring sufficient statistics)
- Equivalently, want to generate signal events with the particular topologies (VBF) we will later select
- Thus before comparing with background, want to impose **MadGraph-level cuts** on signal events
- Two topologies being targeted by our cuts: `g g > ax g g` and `Z/W > j j`

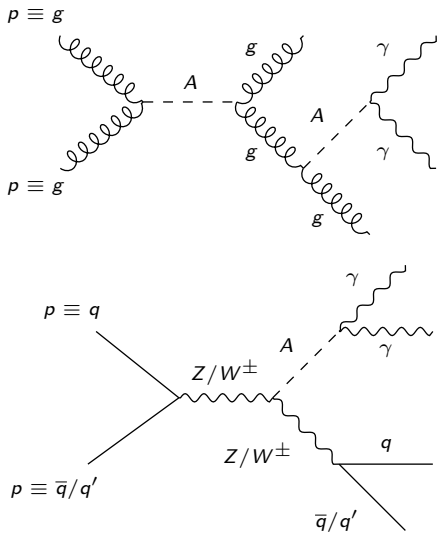

Final Approach

- Choose to generate 1000000 signal events with all of the previous commands/setting, along with the following additional MadGraph selections.

  $|\Delta\eta^{jj}| > 2.4$, $m^{jj} > 120$ GeV
  - The gluon-gluon channel primarily exhibits low $|\Delta\eta^{jj}|$, so we apply a cut there to reduce its cross section
  - As noted, associated axion production satisfies $m^{jj} \approx 80$ GeV, so we apply an m^{jj} cut to reduce that cross section as well

Increasing VBF Purity in Signal

Objective

- Want to generate signal events in a phase space region which emphasizes our eventual optimization (ensuring sufficient statistics)
- Equivalently, want to generate signal events with the particular topologies (VBF) we will later select
- Thus before comparing with background, want to impose **MadGraph-level cuts** on signal events
- Two topologies being targeted by our cuts: `g g > ax g g` and `Z/W > j j`

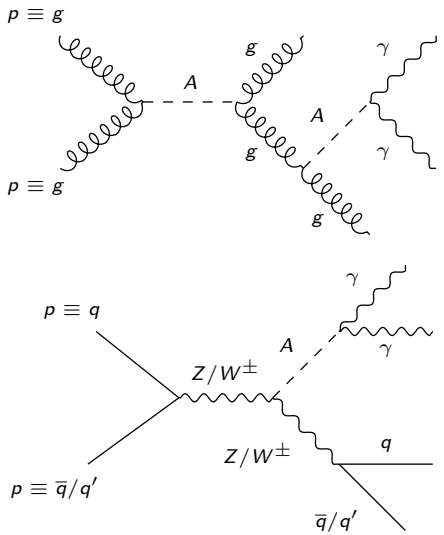

Final Approach

- Choose to generate 1000000 signal events with all of the previous commands/setting, along with the following additional MadGraph selections.

  $|\Delta\eta^{jj}| > 2.4$, $m^{jj} > 120$ GeV
  - The gluon-gluon channel primarily exhibits low $|\Delta\eta^{jj}|$, so we apply a cut there to reduce its cross section
  - As noted, associated axion production satisfies $m^{jj} \approx 80$ GeV, so we apply an m^{jj} cut to reduce that cross section as well
- The cross section for this signal is $0.10235 \pm 2.82\text{e-}5$ pb

Increasing VBF Purity in Signal

Objective

- Want to generate signal events in a phase space region which emphasizes our eventual optimization (ensuring sufficient statistics)
- Equivalently, want to generate signal events with the particular topologies (VBF) we will later select
- Thus before comparing with background, want to impose **MadGraph-level cuts** on signal events
- Two topologies being targeted by our cuts: `g g > ax g g` and `Z/W > j j`

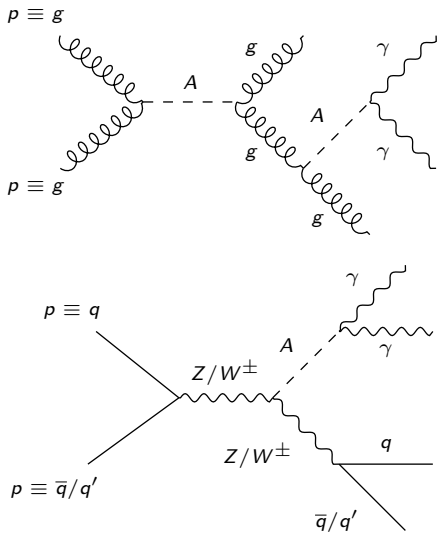

Final Approach

- Choose to generate 1000000 signal events with all of the previous commands/setting, along with the following additional MadGraph selections.

  $|\Delta\eta^{jj}| > 2.4$, $m^{jj} > 120$ GeV
  - The gluon-gluon channel primarily exhibits low $|\Delta\eta^{jj}|$, so we apply a cut there to reduce its cross section
  - As noted, associated axion production satisfies $m^{jj} \approx 80$ GeV, so we apply an m^{jj} cut to reduce that cross section as well
- The cross section for this signal is $0.10235 \pm 2.82\text{e-}5$ pb

Channel	Cross-Section (pb)
`g g > ax g g`	$0.06911 \pm 2.28\text{e-}5$
VBF channel	$0.03324 \pm 5.1\text{e-}5$

Increasing VBF Purity in Signal

Objective

- Want to generate signal events in a phase space region which emphasizes our eventual optimization (ensuring sufficient statistics)
- Equivalently, want to generate signal events with the particular topologies (VBF) we will later select
- Thus before comparing with background, want to impose **MadGraph-level cuts** on signal events
- Two topologies being targeted by our cuts: `g g > ax g g` and `Z/W > j j`

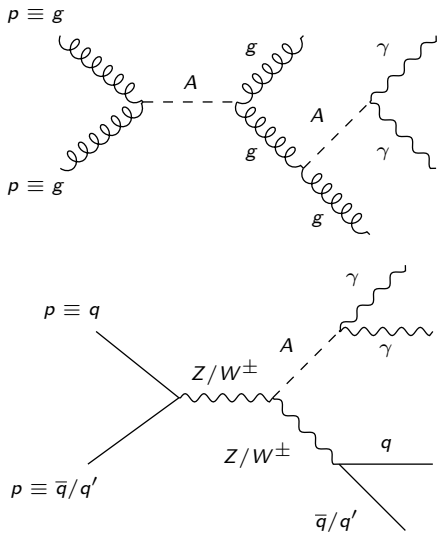

Final Approach

- Choose to generate 1000000 signal events with all of the previous commands/setting, along with the following additional MadGraph selections.

  $|\Delta\eta^{jj}| > 2.4$, $m^{jj} > 120$ GeV
  - The gluon-gluon channel primarily exhibits low $|\Delta\eta^{jj}|$, so we apply a cut there to reduce its cross section
  - As noted, associated axion production satisfies $m^{jj} \approx 80$ GeV, so we apply an m^{jj} cut to reduce that cross section as well
- The cross section for this signal is $0.10235 \pm 2.82\text{e-}5$ pb

Channel	Cross-Section (pb)
`g g > ax g g`	$0.06911 \pm 2.28\text{e-}5$
VBF channel	$0.03324 \pm 5.1\text{e-}5$

- While the gluon-gluon channel still dominates, we've achieved a VBF signal purity sufficient to achieve the necessary statistics during optimization

Background Generation

Background Generation

Process

We're interested in comparing our signal with **two** background processes.

Background Generation

Process

We're interested in comparing our signal with **two** background processes.

- First, a general dijet, diphoton channel generated as follows.

  ```
  generate p p > j j a a
  ```

Background Generation

Process

We're interested in comparing our signal with **two** background processes.

- First, a general dijet, diphoton channel generated as follows.

  `generate p p > j j a a`

- Second, a more specific, VBF-oriented background with no QCD vertices, mimicking our signal generation.

  `generate p p > j j a a QCD=0`

Background Generation

Process

We're interested in comparing our signal with **two** background processes.

- First, a general dijet, diphoton channel generated as follows.

  `generate p p > j j a a`

- Second, a more specific, VBF-oriented background with no QCD vertices, mimicking our signal generation.

  `generate p p > j j a a QCD=0`

- Recognizing our eventual selection of high jet momentum events (VBF jets being boosted by heavy vector boson production), we generate background events in H_T bins

Background Generation

Process

We're interested in comparing our signal with **two** background processes.

- First, a general dijet, diphoton channel generated as follows.

  `generate p p > j j a a`

- Second, a more specific, VBF-oriented background with no QCD vertices, mimicking our signal generation.

  `generate p p > j j a a QCD=0`

- Recognizing our eventual selection of high jet momentum events (VBF jets being boosted by heavy vector boson production), we generate background events in H_T bins
  - In particular, we sought to simulate 1000000 events per background process per each of the following bins (all values given in GeV).

    $[0, 100]$, $[100, 200]$, $[200, 400]$, $[400, 600]$, $[600, 800]$, $[800, 1200]$, $[1200, 1600]$, $[1600, \infty)$

Background Generation

Process

We're interested in comparing our signal with **two** background processes.

- First, a general dijet, diphoton channel generated as follows.

  `generate p p > j j a a`

- Second, a more specific, VBF-oriented background with no QCD vertices, mimicking our signal generation.

  `generate p p > j j a a QCD=0`

- Recognizing our eventual selection of high jet momentum events (VBF jets being boosted by heavy vector boson production), we generate background events in H_T bins
  - In particular, we sought to simulate 1000000 events per background process per each of the following bins (all values given in GeV).

    $[0, 100], [100, 200], [200, 400], [400, 600], [600, 800], [800, 1200], [1200, 1600], [1600, \infty)$

  - MadGraph was unable to produce the full million events for higher H_T bins (likely due to diagram complexity)

Background Generation

Process

We're interested in comparing our signal with **two** background processes.

- First, a general dijet, diphoton channel generated as follows.

  `generate p p > j j a a`

- Second, a more specific, VBF-oriented background with no QCD vertices, mimicking our signal generation.

  `generate p p > j j a a QCD=0`

- Recognizing our eventual selection of high jet momentum events (VBF jets being boosted by heavy vector boson production), we generate background events in H_T bins
  - In particular, we sought to simulate 1000000 events per background process per each of the following bins (all values given in GeV).

    $[0, 100], [100, 200], [200, 400], [400, 600], [600, 800], [800, 1200], [1200, 1600], [1600, \infty)$
  - MadGraph was unable to produce the full million events for higher H_T bins (likely due to diagram complexity)
  - However, the number of events generated was sufficient to reach desired optimization statistics

Background Generation

Process

We're interested in comparing our signal with **two** background processes.

- First, a general dijet, diphoton channel generated as follows.

  `generate p p > j j a a`

- Second, a more specific, VBF-oriented background with no QCD vertices, mimicking our signal generation.

  `generate p p > j j a a QCD=0`

- Recognizing our eventual selection of high jet momentum events (VBF jets being boosted by heavy vector boson production), we generate background events in H_T bins
  - In particular, we sought to simulate 1000000 events per background process per each of the following bins (all values given in GeV).

    $[0, 100], [100, 200], [200, 400], [400, 600], [600, 800], [800, 1200], [1200, 1600], [1600, \infty)$
  - MadGraph was unable to produce the full million events for higher H_T bins (likely due to diagram complexity)
  - However, the number of events generated was sufficient to reach desired optimization statistics
- Prototypical Feynman diagrams are given for the general (left) and QCD $= 0$ (right) cases.

Background Generation

Process

We're interested in comparing our signal with **two** background processes.

- First, a general dijet, diphoton channel generated as follows.

  `generate p p > j j a a`

- Second, a more specific, VBF-oriented background with no QCD vertices, mimicking our signal generation.

  `generate p p > j j a a QCD=0`

- Recognizing our eventual selection of high jet momentum events (VBF jets being boosted by heavy vector boson production), we generate background events in H_T bins
  - In particular, we sought to simulate 1000000 events per background process per each of the following bins (all values given in GeV).

    $[0, 100], [100, 200], [200, 400], [400, 600], [600, 800], [800, 1200], [1200, 1600], [1600, \infty)$
  - MadGraph was unable to produce the full million events for higher H_T bins (likely due to diagram complexity)
  - However, the number of events generated was sufficient to reach desired optimization statistics
- Prototypical Feynman diagrams are given for the general (left) and QCD $= 0$ (right) cases.

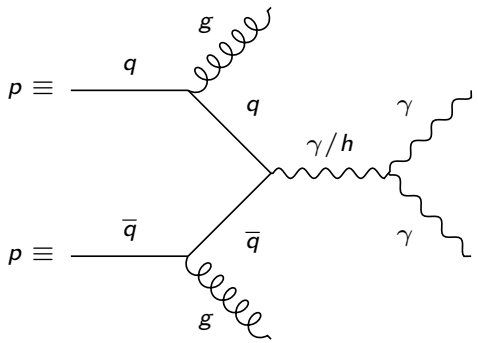

Background Generation

Process

We're interested in comparing our signal with **two** background processes.

- First, a general dijet, diphoton channel generated as follows.

  `generate p p > j j a a`

- Second, a more specific, VBF-oriented background with no QCD vertices, mimicking our signal generation.

  `generate p p > j j a a QCD=0`

- Recognizing our eventual selection of high jet momentum events (VBF jets being boosted by heavy vector boson production), we generate background events in H_T bins
  - In particular, we sought to simulate 1000000 events per background process per each of the following bins (all values given in GeV).

    $[0, 100], [100, 200], [200, 400], [400, 600], [600, 800], [800, 1200], [1200, 1600], [1600, \infty)$
  - MadGraph was unable to produce the full million events for higher H_T bins (likely due to diagram complexity)
  - However, the number of events generated was sufficient to reach desired optimization statistics
- Prototypical Feynman diagrams are given for the general (left) and QCD $= 0$ (right) cases.

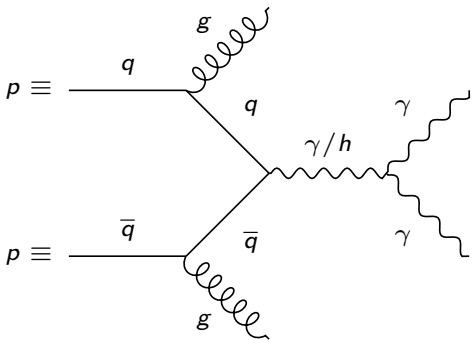

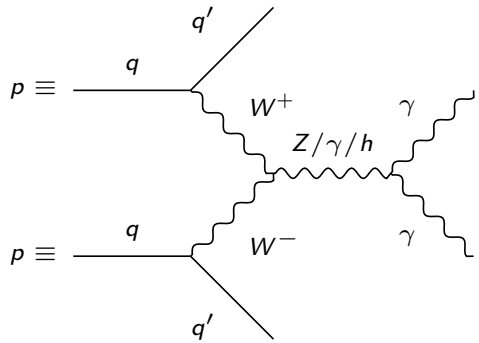

Kinematics with MG-Level Cuts

Kinematics with MG-Level Cuts

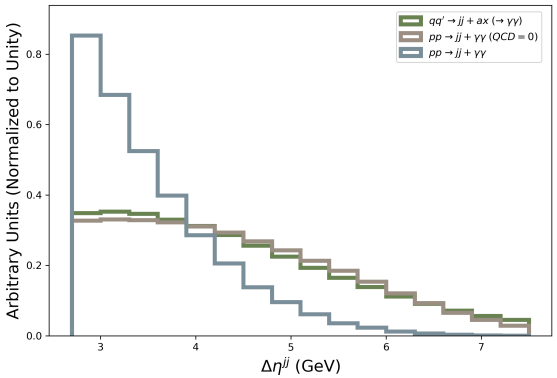

Kinematics with MG-Level Cuts

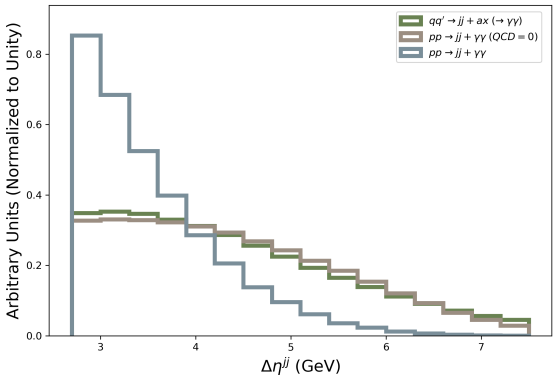

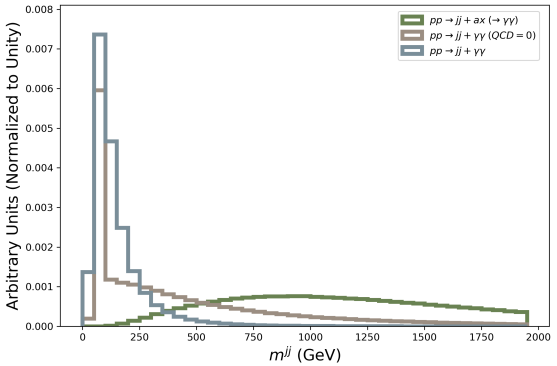

Kinematics with MG-Level Cuts

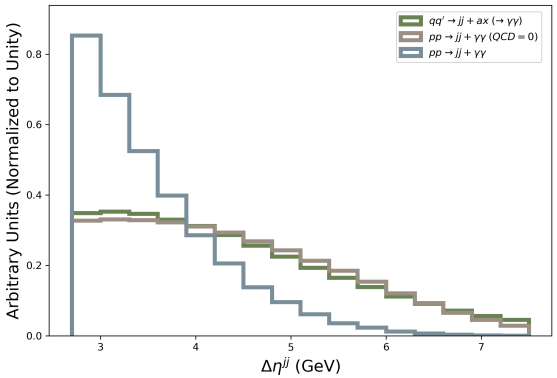

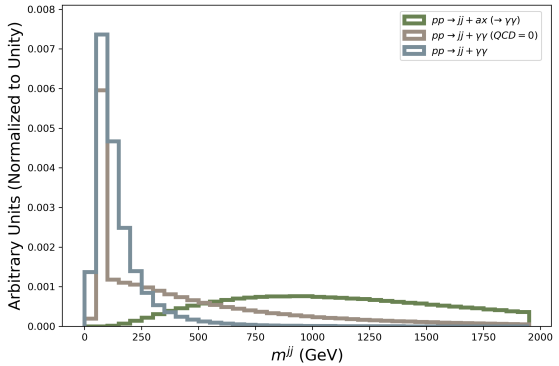

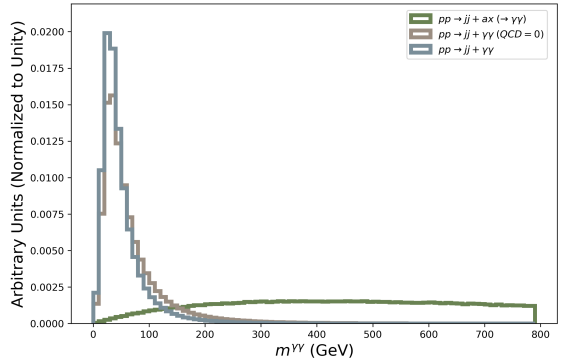

Kinematics with MG-Level Cuts

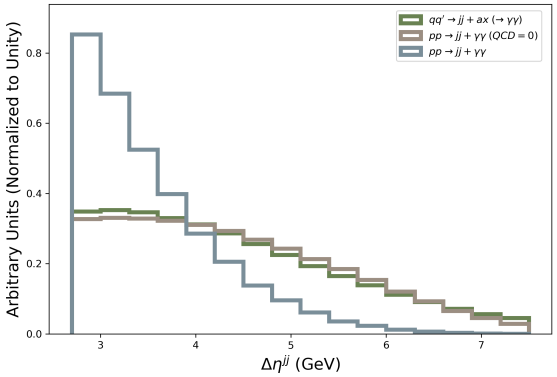

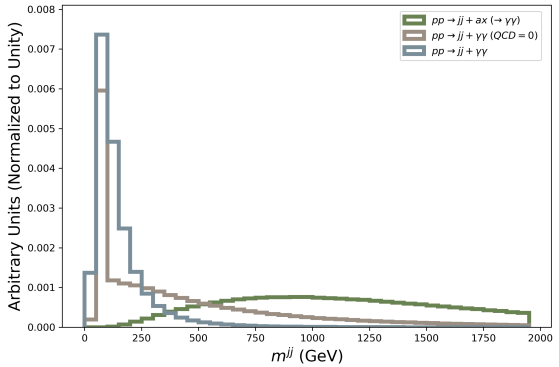

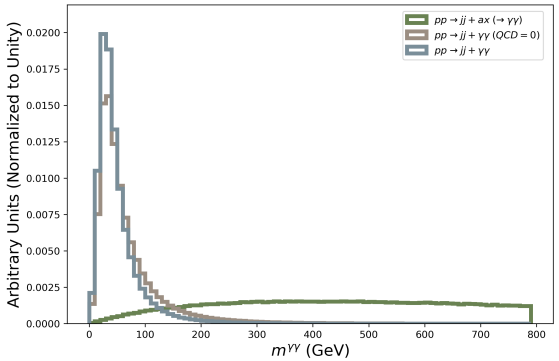

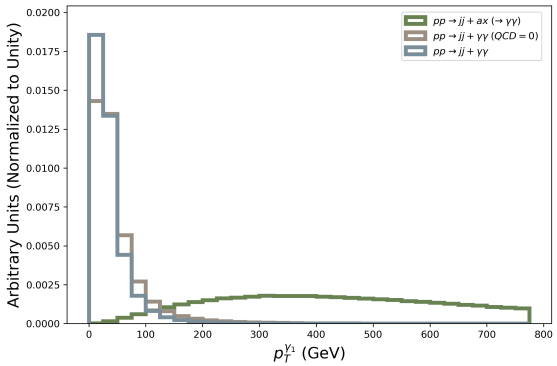

Kinematics with MG-Level Cuts

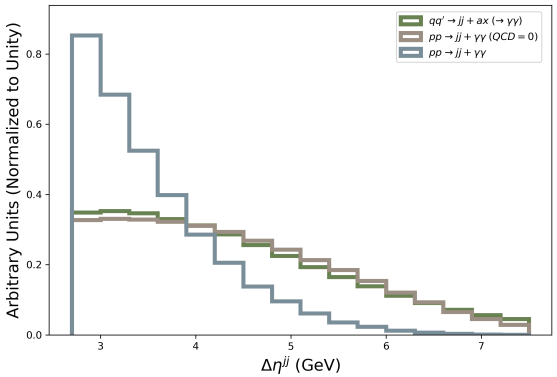

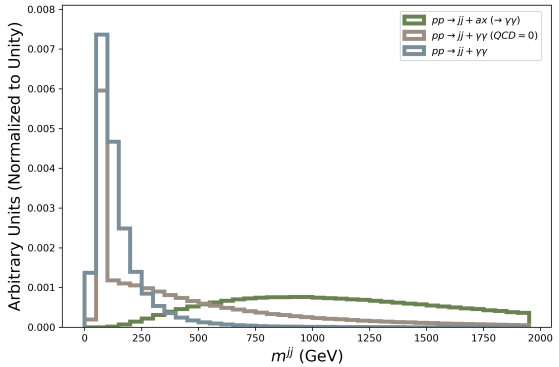

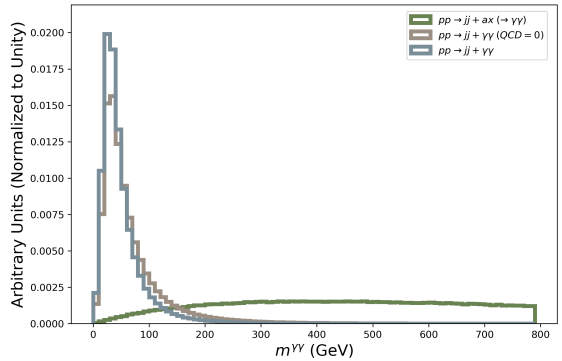

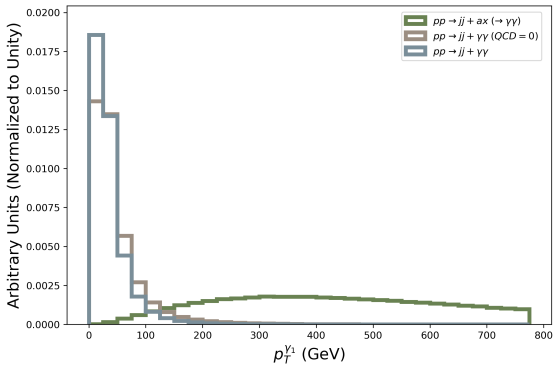

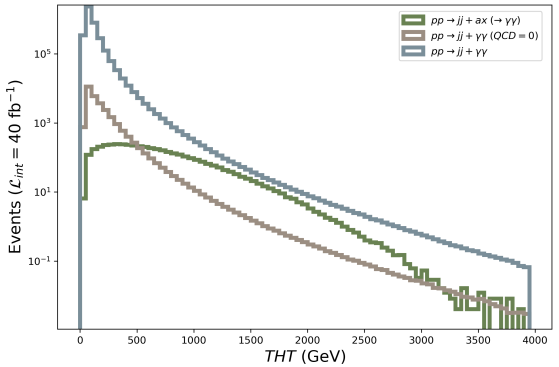

Kinematics with MG-Level Cuts

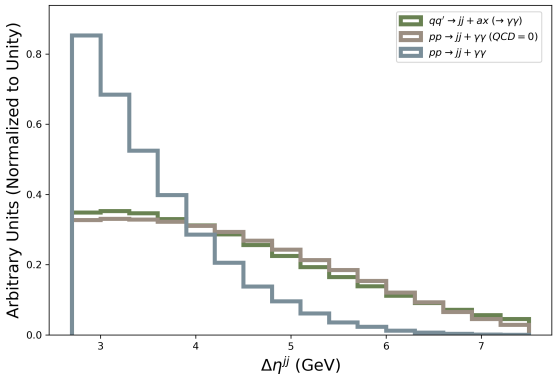

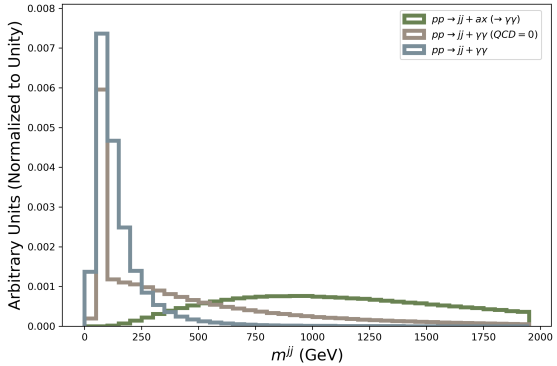

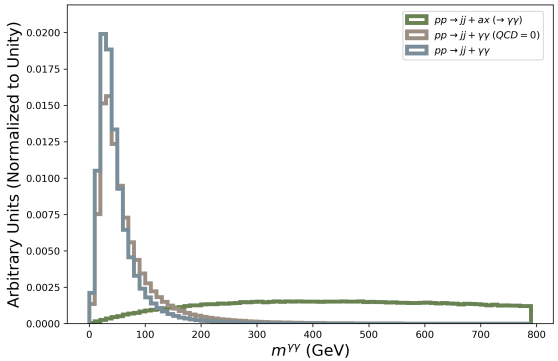

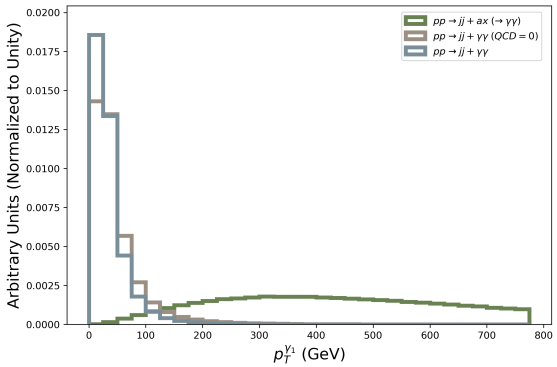

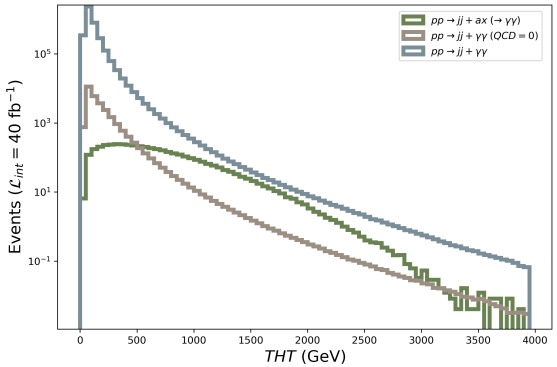

Comments

Kinematics with MG-Level Cuts

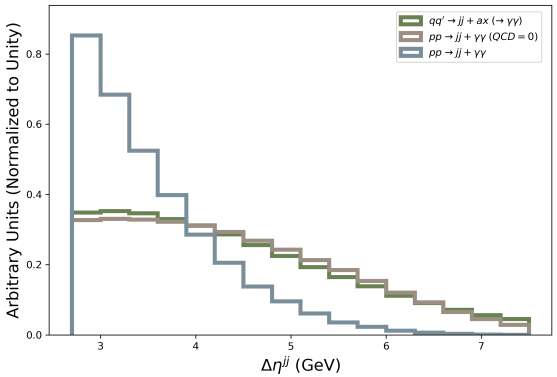

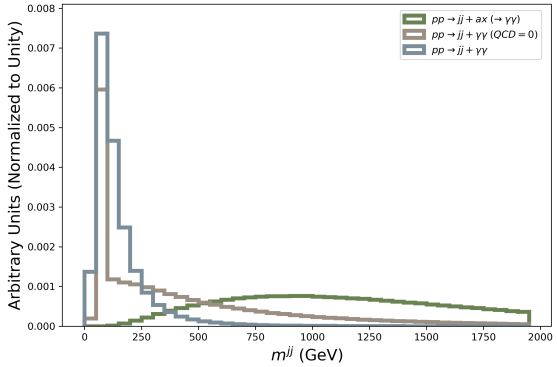

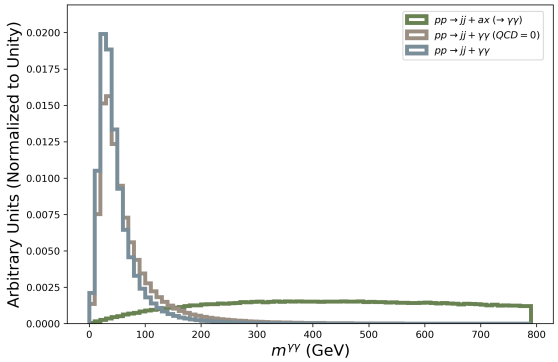

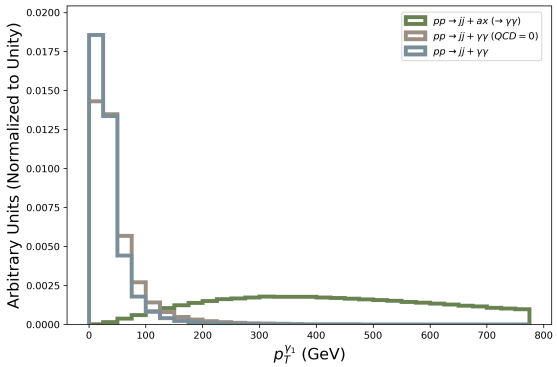

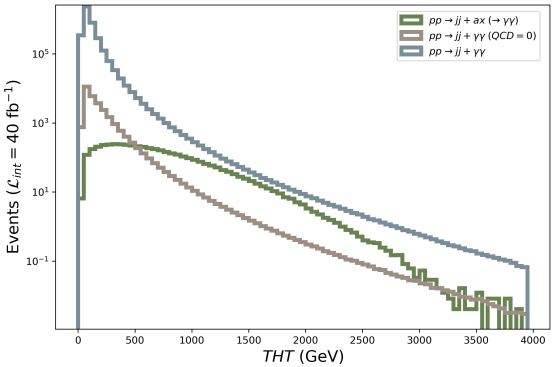

Comments

- First four kinematic plots exhibit high signal-background discriminating power in the variables $\Delta\eta^{jj}$, m^{jj}, $m^{\gamma\gamma}$, p_T^{γ}, motivating our upcoming optimization procedure

Kinematics with MG-Level Cuts

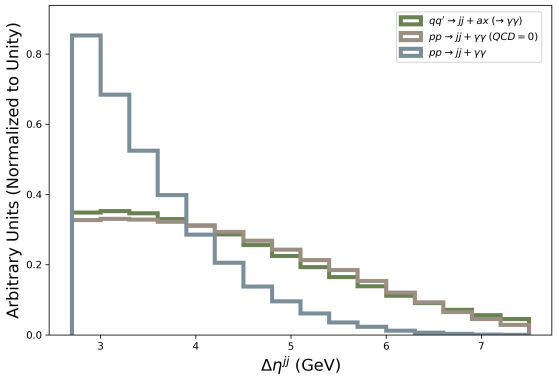

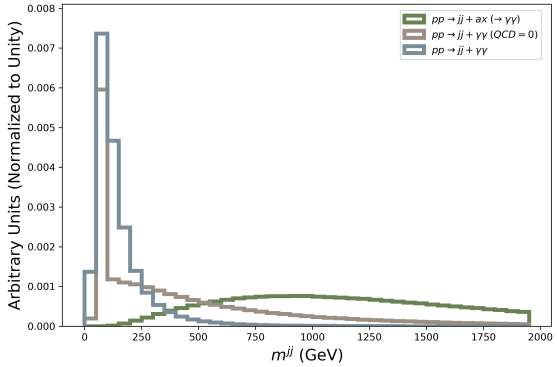

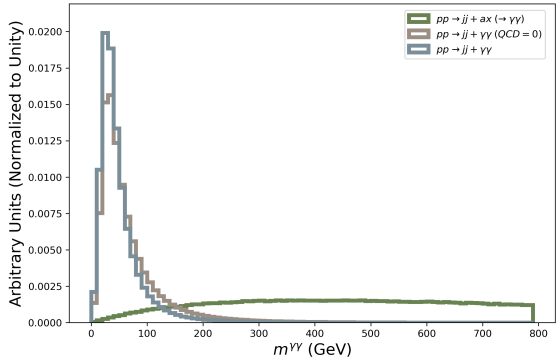

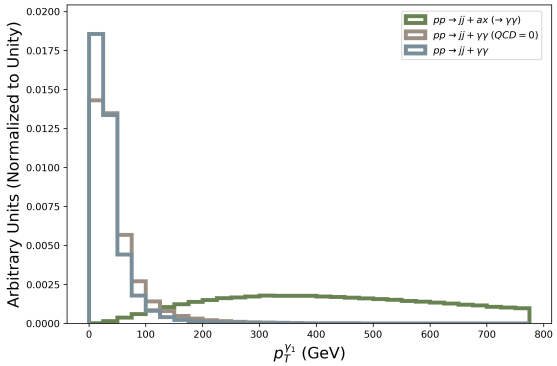

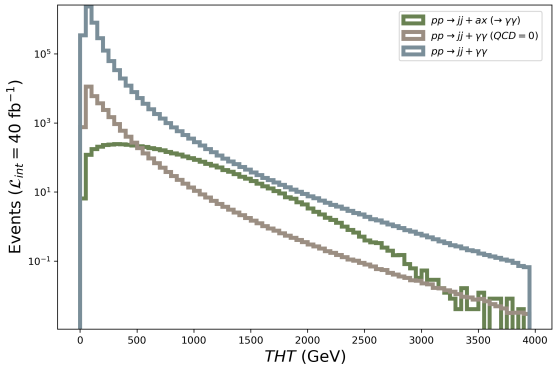

Comments

- First four kinematic plots exhibit high signal-background discriminating power in the variables $\Delta\eta^{jj}$, m^{jj}, $m^{\gamma\gamma}$, p_T^{γ}, motivating our upcoming optimization procedure
  - More subtle in the $\Delta\eta^{jj}$ case: only the VBF subset of the signal has high $\Delta\eta^{jj}$, so disc. power appears only when omitting gluon-gluon signal events (removing g from the MadGraph proton definition)

Kinematics with MG-Level Cuts

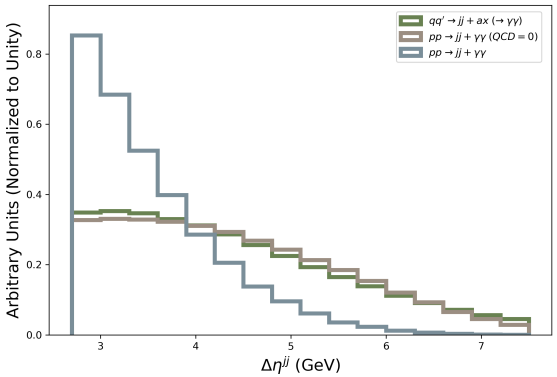

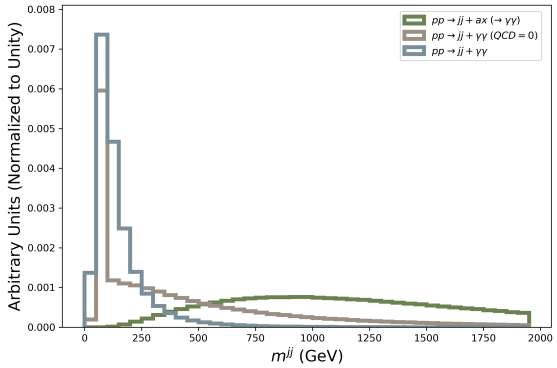

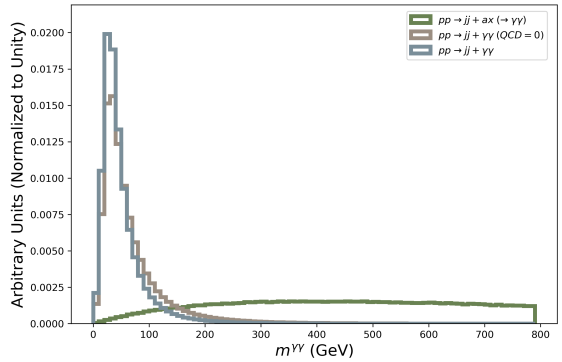

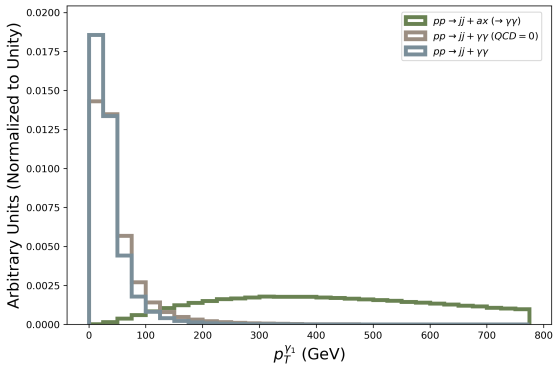

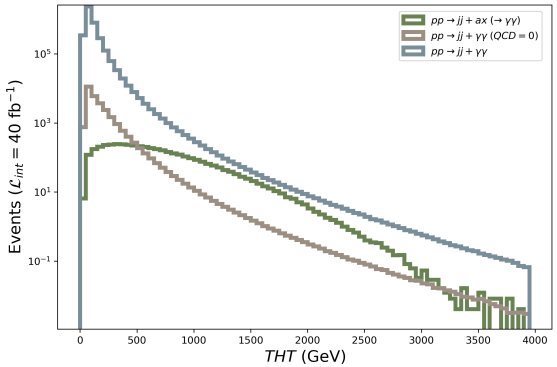

Comments

- First four kinematic plots exhibit high signal-background discriminating power in the variables $\Delta\eta^{jj}$, m^{jj}, $m^{\gamma\gamma}$, p_T^{γ}, motivating our upcoming optimization procedure
  - More subtle in the $\Delta\eta^{jj}$ case: only the VBF subset of the signal has high $\Delta\eta^{jj}$, so disc. power appears only when omitting gluon-gluon signal events (removing g from the MadGraph proton definition)
- The final kinematic plot demonstrates how our H_T-binned background samples are "stiched" together smoothly when normalized to cross section

Jet Variable Selection Optimization ($\Delta\eta^{jj}$, m^{jj})

Jet Variable Selection Optimization ($\Delta\eta^{jj}$, m^{jj})

Process

Jet Variable Selection Optimization ($\Delta\eta^{jj}$, m^{jj})

Process

- Optimized $\Delta\eta^{jj}$ and m^{jj} selections simultaneously (to account for correlations)

Jet Variable Selection Optimization ($\Delta\eta^{jj}$, m^{jj})

Process

- Optimized $\Delta\eta^{jj}$ and m^{jj} selections simultaneously (to account for correlations)
- Performed a gridsearch on pairs of selections $|\Delta\eta^{jj}| > \eta_0$, $m^{jj} > m_0^j$ for the following values (m_0^j given in GeV)

  $(\eta_0, m_0^j) \in \{2.6, 3.1, 3.6, 4.1, 4.6, 5.1, 5.6, 6.1\} \times \{120, 500, 750, 1000, 1250, 1500, 1750, 2000\}$

Jet Variable Selection Optimization ($\Delta\eta^{jj}$, m^{jj})

Process

- Optimized $\Delta\eta^{jj}$ and m^{jj} selections simultaneously (to account for correlations)
- Performed a gridsearch on pairs of selections $|\Delta\eta^{jj}| > \eta_0$, $m^{jj} > m_0^j$ for the following values (m_0^j given in GeV)

  $(\eta_0, m_0^j) \in \{2.6, 3.1, 3.6, 4.1, 4.6, 5.1, 5.6, 6.1\} \times \{120, 500, 750, 1000, 1250, 1500, 1750, 2000\}$
- Significance computed twice on each of $8 \cdot 8 = 64$ scenarios: without (left) and with (right) systematic uncertainty

Jet Variable Selection Optimization ($\Delta\eta^{jj}$, m^{jj})

Process

- Optimized $\Delta\eta^{jj}$ and m^{jj} selections simultaneously (to account for correlations)
- Performed a gridsearch on pairs of selections $|\Delta\eta^{jj}| > \eta_0$, $m^{jj} > m_0^j$ for the following values (m_0^j given in GeV)

  $(\eta_0, m_0^j) \in \{2.6, 3.1, 3.6, 4.1, 4.6, 5.1, 5.6, 6.1\} \times \{120, 500, 750, 1000, 1250, 1500, 1750, 2000\}$
- Significance computed twice on each of $8 \cdot 8 = 64$ scenarios: without (left) and with (right) systematic uncertainty
  - To avoid misleadingly high significance for insufficient signal statistics, we chose $\frac{S}{\sqrt{S+B}}$ over $\frac{S}{B}$

Jet Variable Selection Optimization ($\Delta\eta^{jj}$, m^{jj})

Process

- Optimized $\Delta\eta^{jj}$ and m^{jj} selections simultaneously (to account for correlations)
- Performed a gridsearch on pairs of selections $|\Delta\eta^{jj}| > \eta_0$, $m^{jj} > m_0^j$ for the following values (m_0^j given in GeV)

  $(\eta_0, m_0^j) \in \{2.6, 3.1, 3.6, 4.1, 4.6, 5.1, 5.6, 6.1\} \times \{120, 500, 750, 1000, 1250, 1500, 1750, 2000\}$
- Significance computed twice on each of $8 \cdot 8 = 64$ scenarios: without (left) and with (right) systematic uncertainty
  - To avoid misleadingly high significance for insufficient signal statistics, we chose $\frac{S}{\sqrt{S+B}}$ over $\frac{S}{B}$
  - Systematic uncertainty approximation then implemented via denominator term $(r \cdot B)^2$ for $r \in [0, 1]$

Jet Variable Selection Optimization ($\Delta\eta^{jj}$, m^{jj})

Process

- Optimized $\Delta\eta^{jj}$ and m^{jj} selections simultaneously (to account for correlations)
- Performed a gridsearch on pairs of selections $|\Delta\eta^{jj}| > \eta_0$, $m^{jj} > m_0^j$ for the following values (m_0^j given in GeV)

  $(\eta_0, m_0^j) \in \{2.6, 3.1, 3.6, 4.1, 4.6, 5.1, 5.6, 6.1\} \times \{120, 500, 750, 1000, 1250, 1500, 1750, 2000\}$
- Significance computed twice on each of $8 \cdot 8 = 64$ scenarios: without (left) and with (right) systematic uncertainty
  - To avoid misleadingly high significance for insufficient signal statistics, we chose $\frac{S}{\sqrt{S+B}}$ over $\frac{S}{B}$
  - Systematic uncertainty approximation then implemented via denominator term $(r \cdot B)^2$ for $r \in [0, 1]$

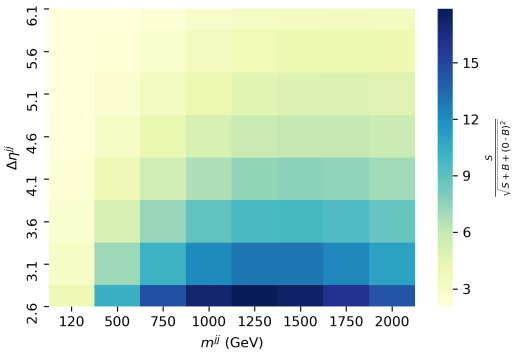

Jet Variable Selection Optimization ($\Delta\eta^{jj}$, m^{jj})

Process

- Optimized $\Delta\eta^{jj}$ and m^{jj} selections simultaneously (to account for correlations)
- Performed a gridsearch on pairs of selections $|\Delta\eta^{jj}| > \eta_0$, $m^{jj} > m_0^j$ for the following values (m_0^j given in GeV)

  $(\eta_0, m_0^j) \in \{2.6, 3.1, 3.6, 4.1, 4.6, 5.1, 5.6, 6.1\} \times \{120, 500, 750, 1000, 1250, 1500, 1750, 2000\}$
- Significance computed twice on each of $8 \cdot 8 = 64$ scenarios: without (left) and with (right) systematic uncertainty
  - To avoid misleadingly high significance for insufficient signal statistics, we chose $\frac{S}{\sqrt{S+B}}$ over $\frac{S}{B}$
  - Systematic uncertainty approximation then implemented via denominator term $(r \cdot B)^2$ for $r \in [0, 1]$

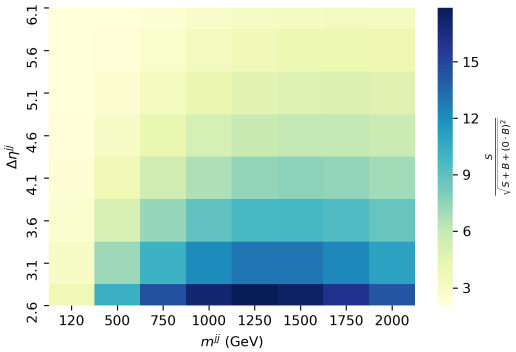

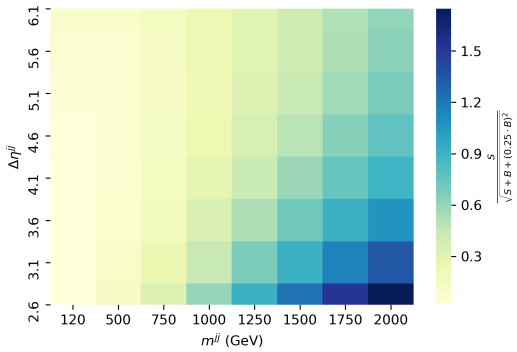

Jet Variable Selection Optimization ($\Delta\eta^{jj}$, m^{jj})

Process

- Optimized $\Delta\eta^{jj}$ and m^{jj} selections simultaneously (to account for correlations)
- Performed a gridsearch on pairs of selections $|\Delta\eta^{jj}| > \eta_0$, $m^{jj} > m_0^j$ for the following values (m_0^j given in GeV)

  $(\eta_0, m_0^j) \in \{2.6, 3.1, 3.6, 4.1, 4.6, 5.1, 5.6, 6.1\} \times \{120, 500, 750, 1000, 1250, 1500, 1750, 2000\}$
- Significance computed twice on each of $8 \cdot 8 = 64$ scenarios: without (left) and with (right) systematic uncertainty
  - To avoid misleadingly high significance for insufficient signal statistics, we chose $\frac{S}{\sqrt{S+B}}$ over $\frac{S}{B}$
  - Systematic uncertainty approximation then implemented via denominator term $(r \cdot B)^2$ for $r \in [0, 1]$

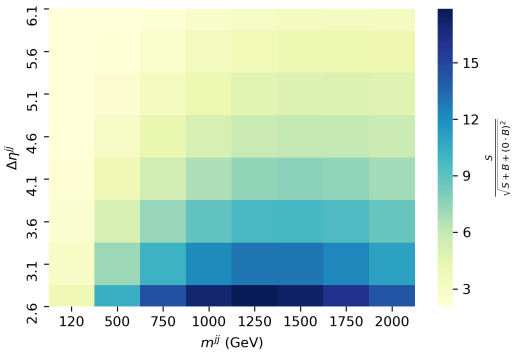

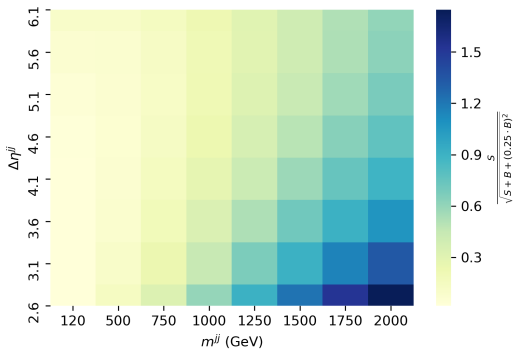

Conclusions

Experimental constraints motivate prioritizing higher $\Delta\eta^{jj}$ cuts, and our sys. uncert. approximation fails at higher m^{jj} cuts, so we invoke the non-sys. uncert. results and pursue two selection pairs:

Jet Variable Selection Optimization ($\Delta\eta^{jj}$, m^{jj})

Process

- Optimized $\Delta\eta^{jj}$ and m^{jj} selections simultaneously (to account for correlations)
- Performed a gridsearch on pairs of selections $|\Delta\eta^{jj}| > \eta_0$, $m^{jj} > m_0^j$ for the following values (m_0^j given in GeV)

  $(\eta_0, m_0^j) \in \{2.6, 3.1, 3.6, 4.1, 4.6, 5.1, 5.6, 6.1\} \times \{120, 500, 750, 1000, 1250, 1500, 1750, 2000\}$
- Significance computed twice on each of $8 \cdot 8 = 64$ scenarios: without (left) and with (right) systematic uncertainty
  - To avoid misleadingly high significance for insufficient signal statistics, we chose $\frac{S}{\sqrt{S+B}}$ over $\frac{S}{B}$
  - Systematic uncertainty approximation then implemented via denominator term $(r \cdot B)^2$ for $r \in [0, 1]$

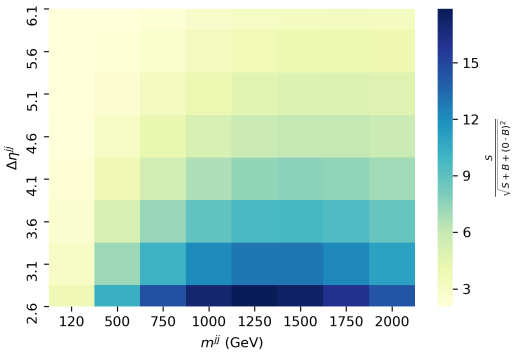

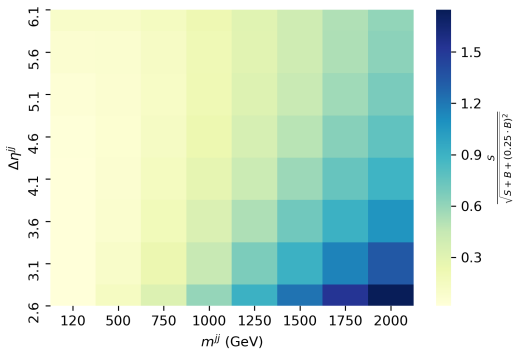

Conclusions

Experimental constraints motivate prioritizing higher $\Delta\eta^{jj}$ cuts, and our sys. uncert. approximation fails at higher m^{jj} cuts, so we invoke the non-sys. uncert. results and pursue two selection pairs:

- A tight (lower significance/more experimental feasibility) cut $(\eta_0, m_0^j) = (3.6, 1250)$

Jet Variable Selection Optimization ($\Delta\eta^{jj}$, m^{jj})

Process

- Optimized $\Delta\eta^{jj}$ and m^{jj} selections simultaneously (to account for correlations)
- Performed a gridsearch on pairs of selections $|\Delta\eta^{jj}| > \eta_0$, $m^{jj} > m_0^j$ for the following values (m_0^j given in GeV)

  $(\eta_0, m_0^j) \in \{2.6, 3.1, 3.6, 4.1, 4.6, 5.1, 5.6, 6.1\} \times \{120, 500, 750, 1000, 1250, 1500, 1750, 2000\}$
- Significance computed twice on each of $8 \cdot 8 = 64$ scenarios: without (left) and with (right) systematic uncertainty
  - To avoid misleadingly high significance for insufficient signal statistics, we chose $\frac{S}{\sqrt{S+B}}$ over $\frac{S}{B}$
  - Systematic uncertainty approximation then implemented via denominator term $(r \cdot B)^2$ for $r \in [0, 1]$

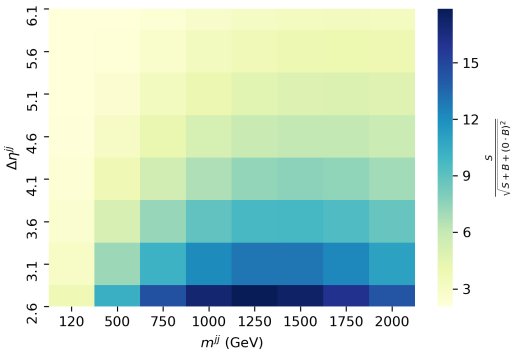

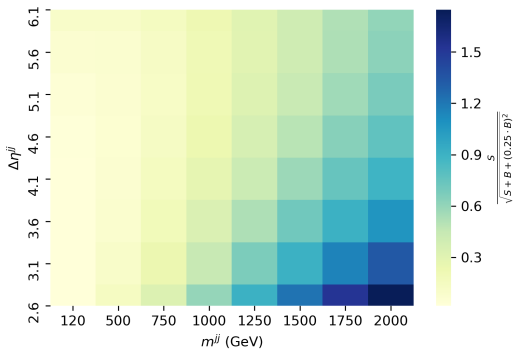

Conclusions

Experimental constraints motivate prioritizing higher $\Delta\eta^{jj}$ cuts, and our sys. uncert. approximation fails at higher m^{jj} cuts, so we invoke the non-sys. uncert. results and pursue two selection pairs:

- A tight (lower significance/more experimental feasibility) cut $(\eta_0, m_0^j) = (3.6, 1250)$
- A loose (higher significance/less experimental feasibility) cut $(\eta_0, m_0^j) = (2.6, 1250)$

Checking Photon Discriminating Power

Checking Photon Discriminating Power

Objective

Before proceeding to the optimization for the other two variables—$m^{\gamma\gamma}$, p_T^{γ}—we check that our tight/loose $\Delta\eta^{jj}$, m^{jj} selections haven't reduced the photon variable discriminating power.

Checking Photon Discriminating Power

Objective

Before proceeding to the optimization for the other two variables—$m^{\gamma\gamma}$, p_T^{γ}—we check that our tight/loose $\Delta\eta^{jj}$, m^{jj} selections haven't reduced the photon variable discriminating power.

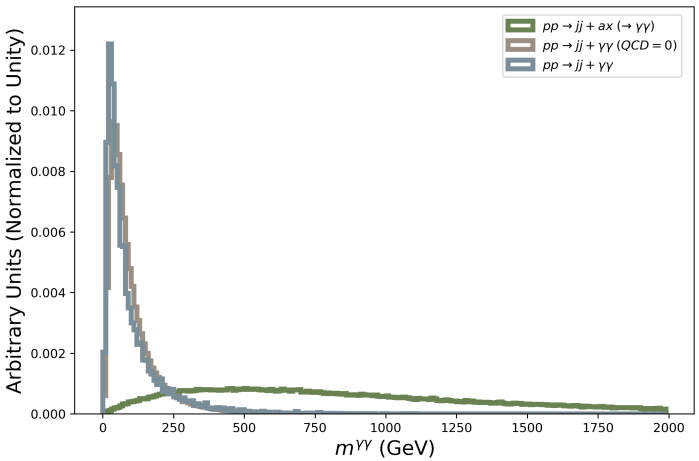

Checking Photon Discriminating Power

Objective

Before proceeding to the optimization for the other two variables—$m^{\gamma\gamma}$, p_T^{γ}—we check that our tight/loose $\Delta\eta^{jj}$, m^{jj} selections haven't reduced the photon variable discriminating power.

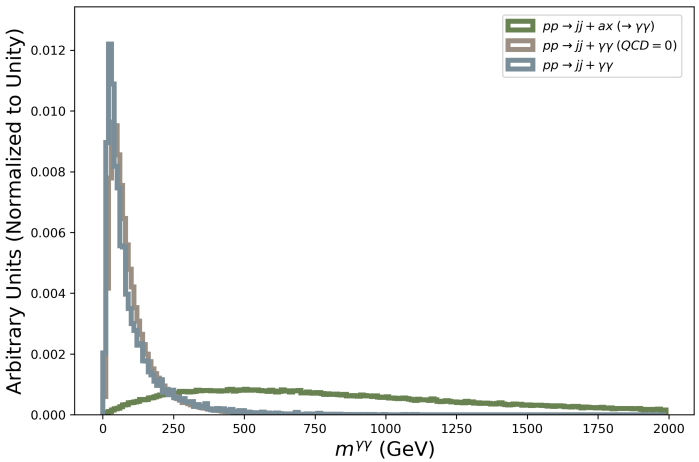

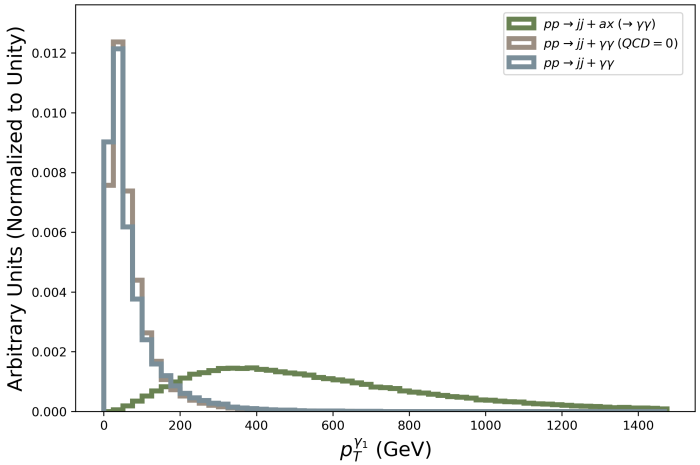

Checking Photon Discriminating Power

Objective

Before proceeding to the optimization for the other two variables—$m^{\gamma\gamma}$, p_T^{γ}—we check that our tight/loose $\Delta\eta^{jj}$, m^{jj} selections haven't reduced the photon variable discriminating power.

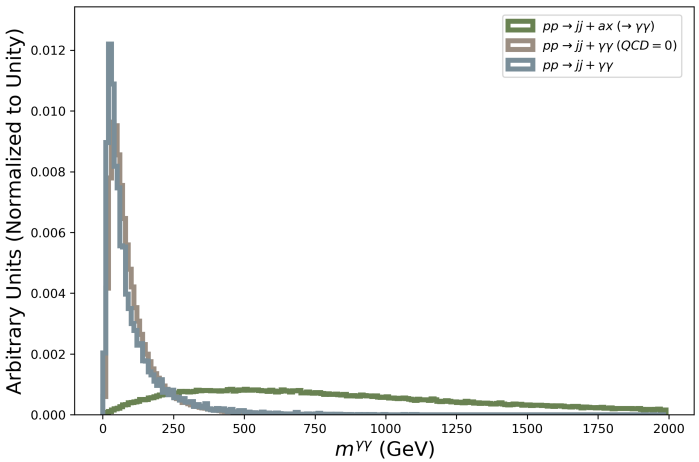

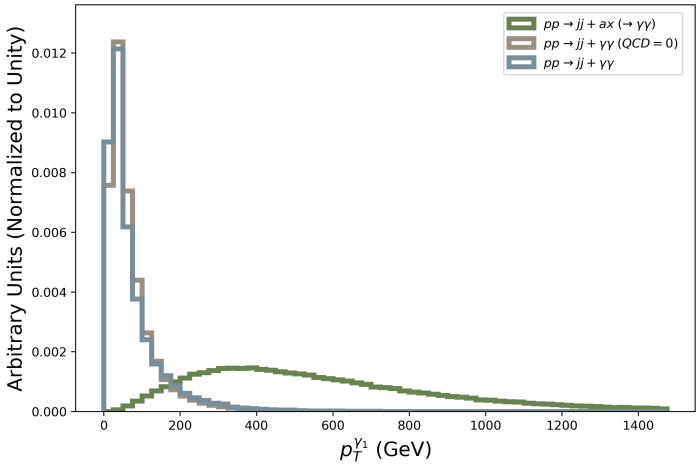

Conclusions

These are "tight cut" plots, but they behave similarly in the loose cuts scenario: thus, discriminating power has been preserved and we can continue onto a photon kinematics optimization routine.

Photon Variable Selection Optimization ($m^{\gamma\gamma}$, p_T^{γ})

Photon Variable Selection Optimization ($m^{\gamma\gamma}$, p_T^{γ})

Process

Photon Variable Selection Optimization ($m^{\gamma\gamma}$, p_T^{γ})

Process

- Optimized $m^{\gamma\gamma}$ and p_T^{γ} selections simultaneously, performing a gridsearch on pairs of selections $m^{\gamma\gamma} > m_0^{\gamma}$, $p_T^{\gamma} > \gamma_0$ on the following values (both variables in GeV)

  $(m_0^{\gamma}, \gamma_0) \in \{200, 250, 300, 350, 400, 450, 500, 550, 600, 650, 700\} \times \{100, 150, 200, 250, 300, 350, 400, 450, 500\}$

Photon Variable Selection Optimization ($m^{\gamma\gamma}$, p_T^{γ})

Process

- Optimized $m^{\gamma\gamma}$ and p_T^{γ} selections simultaneously, performing a gridsearch on pairs of selections $m^{\gamma\gamma} > m_0^{\gamma}$, $p_T^{\gamma} > \gamma_0$ on the following values (both variables in GeV)

  $(m_0^{\gamma}, \gamma_0) \in \{200, 250, 300, 350, 400, 450, 500, 550, 600, 650, 700\} \times \{100, 150, 200, 250, 300, 350, 400, 450, 500\}$
- Computed significance in two ways on each of the $11 \cdot 9 = 99$ scenarios–in particular, using different systematic uncertainty coefficients–for both the tight (left plots) and loose (right plots) selections.

Photon Variable Selection Optimization ($m^{\gamma\gamma}$, p_T^{γ})

Process

- Optimized $m^{\gamma\gamma}$ and p_T^{γ} selections simultaneously, performing a gridsearch on pairs of selections $m^{\gamma\gamma} > m_0^{\gamma}$, $p_T^{\gamma} > \gamma_0$ on the following values (both variables in GeV)

  $(m_0^{\gamma}, \gamma_0) \in \{200, 250, 300, 350, 400, 450, 500, 550, 600, 650, 700\} \times \{100, 150, 200, 250, 300, 350, 400, 450, 500\}$
- Computed significance in two ways on each of the $11 \cdot 9 = 99$ scenarios–in particular, using different systematic uncertainty coefficients–for both the tight (left plots) and loose (right plots) selections.

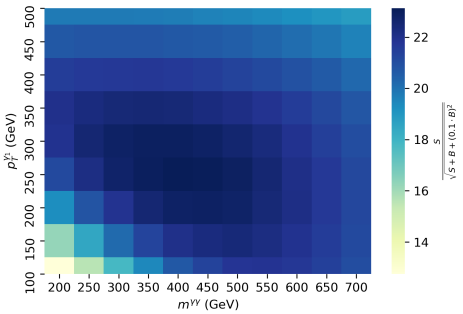

Photon Variable Selection Optimization ($m^{\gamma\gamma}$, p_T^{γ})

Process

- Optimized $m^{\gamma\gamma}$ and p_T^{γ} selections simultaneously, performing a gridsearch on pairs of selections $m^{\gamma\gamma} > m_0^{\gamma}$, $p_T^{\gamma} > \gamma_0$ on the following values (both variables in GeV)

  $(m_0^{\gamma}, \gamma_0) \in \{200, 250, 300, 350, 400, 450, 500, 550, 600, 650, 700\} \times \{100, 150, 200, 250, 300, 350, 400, 450, 500\}$
- Computed significance in two ways on each of the $11 \cdot 9 = 99$ scenarios–in particular, using different systematic uncertainty coefficients–for both the tight (left plots) and loose (right plots) selections.

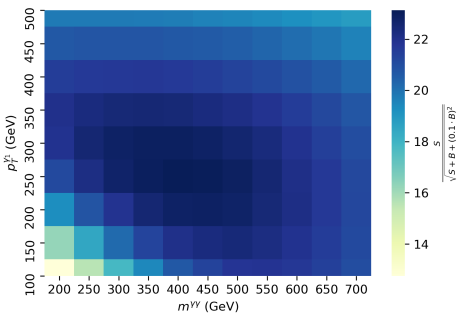

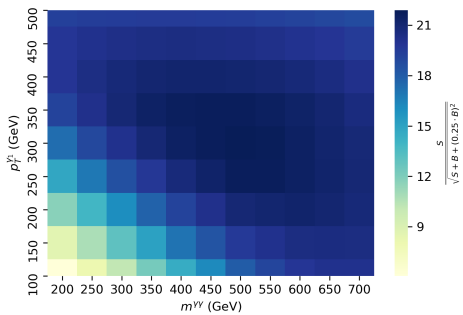

Photon Variable Selection Optimization ($m^{\gamma\gamma}$, p_T^{γ})

Process

- Optimized $m^{\gamma\gamma}$ and p_T^{γ} selections simultaneously, performing a gridsearch on pairs of selections $m^{\gamma\gamma} > m_0^{\gamma}$, $p_T^{\gamma} > \gamma_0$ on the following values (both variables in GeV)

  $(m_0^{\gamma}, \gamma_0) \in \{200, 250, 300, 350, 400, 450, 500, 550, 600, 650, 700\} \times \{100, 150, 200, 250, 300, 350, 400, 450, 500\}$
- Computed significance in two ways on each of the $11 \cdot 9 = 99$ scenarios–in particular, using different systematic uncertainty coefficients–for both the tight (left plots) and loose (right plots) selections.

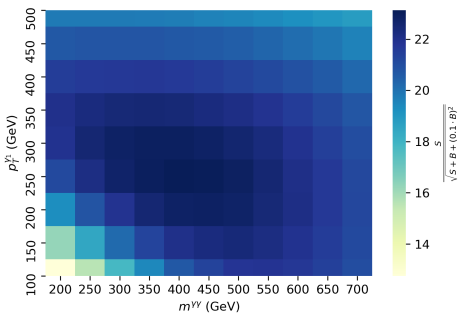

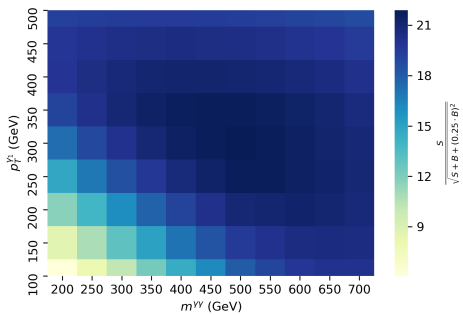

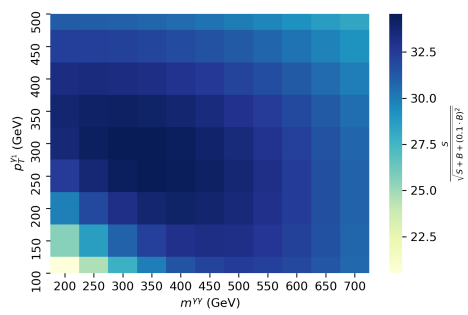

Photon Variable Selection Optimization ($m^{\gamma\gamma}$, p_T^{γ})

Process

- Optimized $m^{\gamma\gamma}$ and p_T^{γ} selections simultaneously, performing a gridsearch on pairs of selections $m^{\gamma\gamma} > m_0^{\gamma}$, $p_T^{\gamma} > \gamma_0$ on the following values (both variables in GeV)

  $(m_0^{\gamma}, \gamma_0) \in \{200, 250, 300, 350, 400, 450, 500, 550, 600, 650, 700\} \times \{100, 150, 200, 250, 300, 350, 400, 450, 500\}$
- Computed significance in two ways on each of the $11 \cdot 9 = 99$ scenarios–in particular, using different systematic uncertainty coefficients–for both the tight (left plots) and loose (right plots) selections.

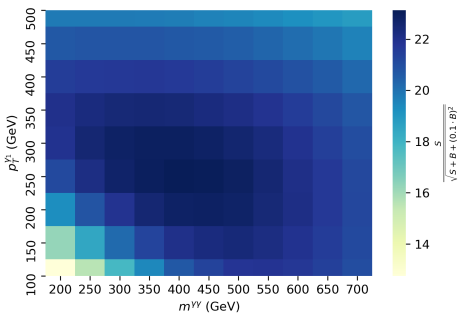

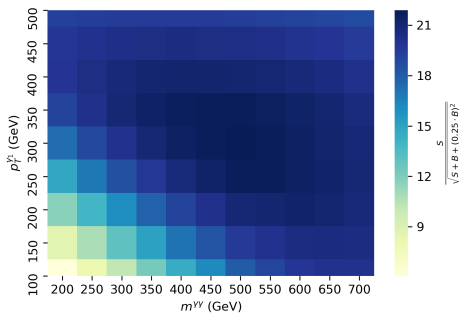

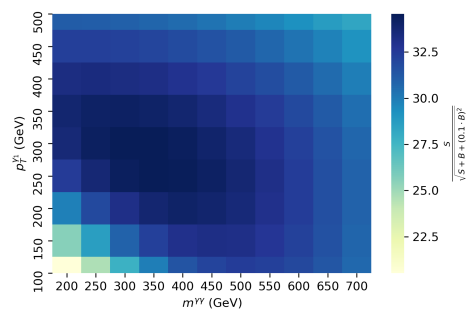

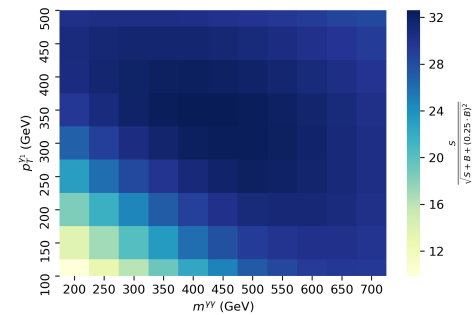

Photon Variable Selection Optimization ($m^{\gamma\gamma}$, p_T^{γ})

Process

- Optimized $m^{\gamma\gamma}$ and p_T^{γ} selections simultaneously, performing a gridsearch on pairs of selections $m^{\gamma\gamma} > m_0^{\gamma}$, $p_T^{\gamma} > \gamma_0$ on the following values (both variables in GeV)

  $(m_0^{\gamma}, \gamma_0) \in \{200, 250, 300, 350, 400, 450, 500, 550, 600, 650, 700\} \times \{100, 150, 200, 250, 300, 350, 400, 450, 500\}$
- Computed significance in two ways on each of the $11 \cdot 9 = 99$ scenarios–in particular, using different systematic uncertainty coefficients–for both the tight (left plots) and loose (right plots) selections.

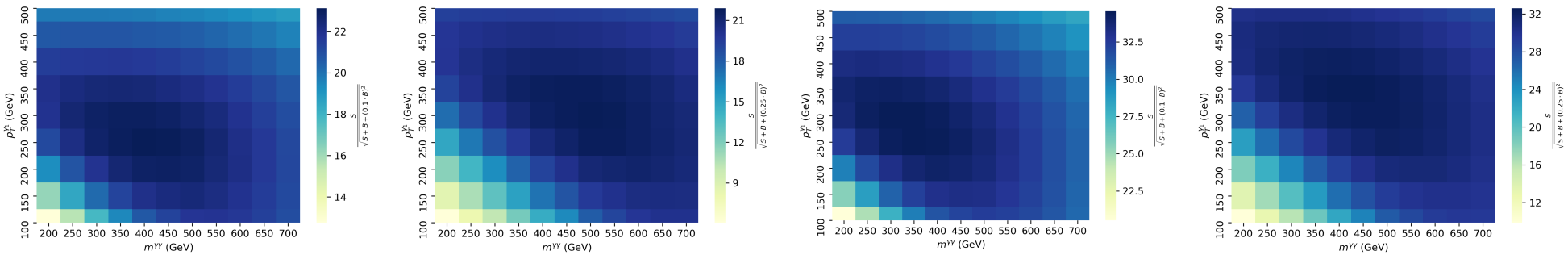

Conclusions

Each heatmap provides us with a slightly different local maxima for significance: we therefore decide to pursue four (m_0^{γ}, γ_0) selections (ordering coinciding with the heatmap ordering).

$$(m_0^{\gamma}, \gamma_0) \in \{(400, 250), (500, 300), (350, 250), (400, 350)\}$$

Jet Variable Selection Optimization, Again ($\Delta\eta^{jj}$, m^{jj})

Jet Variable Selection Optimization, Again ($\Delta\eta^{jj}$, m^{jj})

Process

Jet Variable Selection Optimization, Again ($\Delta\eta^{jj}$, m^{jj})

Process

- Returned to the jet variables to study significance in $\Delta\eta^{jj}$, m^{jj} phase space for each of our four pairs of $m^{\gamma\gamma}$, p_T^{γ} cuts

Jet Variable Selection Optimization, Again ($\Delta\eta^{jj}$, m^{jj})

Process

- Returned to the jet variables to study significance in $\Delta\eta^{jj}$, m^{jj} phase space for each of our four pairs of $m^{\gamma\gamma}$, p_T^{γ} cuts
- Performed smaller gridsearch, with selection pairs $|\Delta\eta^{jj}| > \eta_1$, $m^{jj} > m_1^j$ in the following values (m_1^j also in GeV)

  $(\eta_1, m_1^j) \in \{2.6, 3.1, 3.6, 4.1\} \times \{750, 1000, 1250, 1500, 1750, 2000\}$

Jet Variable Selection Optimization, Again ($\Delta\eta^{jj}$, m^{jj})

Process

- Returned to the jet variables to study significance in $\Delta\eta^{jj}$, m^{jj} phase space for each of our four pairs of $m^{\gamma\gamma}$, p_T^{γ} cuts
- Performed smaller gridsearch, with selection pairs $|\Delta\eta^{jj}| > \eta_1$, $m^{jj} > m_1^j$ in the following values (m_1^j also in GeV)

  $(\eta_1, m_1^j) \in \{2.6, 3.1, 3.6, 4.1\} \times \{750, 1000, 1250, 1500, 1750, 2000\}$
- Computed significance just once on each of these $4 \cdot 6 = 24$ scenarios, using the systematic uncertainty coefficient which led to the choice of that particular $m^{\gamma\gamma}$, p_T^{γ} selection; plots are ordered as follows

  $(m_0^{\gamma}, \gamma_0) = (400, 250), (m_0^{\gamma}, \gamma_0) = (500, 300), (m_0^{\gamma}, \gamma_0) = (350, 250), (m_0^{\gamma}, \gamma_0) = (400, 350)$

Jet Variable Selection Optimization, Again ($\Delta\eta^{jj}$, m^{jj})

Process

- Returned to the jet variables to study significance in $\Delta\eta^{jj}$, m^{jj} phase space for each of our four pairs of $m^{\gamma\gamma}$, p_T^{γ} cuts
- Performed smaller gridsearch, with selection pairs $|\Delta\eta^{jj}| > \eta_1$, $m^{jj} > m_1^j$ in the following values (m_1^j also in GeV)

  $(\eta_1, m_1^j) \in \{2.6, 3.1, 3.6, 4.1\} \times \{750, 1000, 1250, 1500, 1750, 2000\}$
- Computed significance just once on each of these $4 \cdot 6 = 24$ scenarios, using the systematic uncertainty coefficient which led to the choice of that particular $m^{\gamma\gamma}$, p_T^{γ} selection; plots are ordered as follows

  $(m_0^{\gamma}, \gamma_0) = (400, 250), (m_0^{\gamma}, \gamma_0) = (500, 300), (m_0^{\gamma}, \gamma_0) = (350, 250), (m_0^{\gamma}, \gamma_0) = (400, 350)$

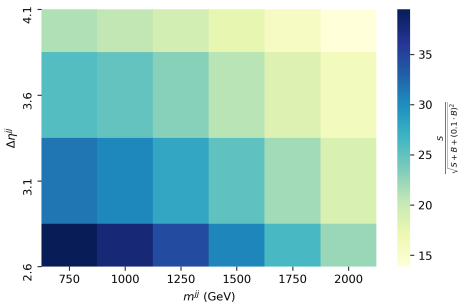

Jet Variable Selection Optimization, Again ($\Delta\eta^{jj}$, m^{jj})

Process

- Returned to the jet variables to study significance in $\Delta\eta^{jj}$, m^{jj} phase space for each of our four pairs of $m^{\gamma\gamma}$, p_T^{γ} cuts
- Performed smaller gridsearch, with selection pairs $|\Delta\eta^{jj}| > \eta_1$, $m^{jj} > m_1^j$ in the following values (m_1^j also in GeV)

  $(\eta_1, m_1^j) \in \{2.6, 3.1, 3.6, 4.1\} \times \{750, 1000, 1250, 1500, 1750, 2000\}$
- Computed significance just once on each of these $4 \cdot 6 = 24$ scenarios, using the systematic uncertainty coefficient which led to the choice of that particular $m^{\gamma\gamma}$, p_T^{γ} selection; plots are ordered as follows

  $(m_0^{\gamma}, \gamma_0) = (400, 250), (m_0^{\gamma}, \gamma_0) = (500, 300), (m_0^{\gamma}, \gamma_0) = (350, 250), (m_0^{\gamma}, \gamma_0) = (400, 350)$

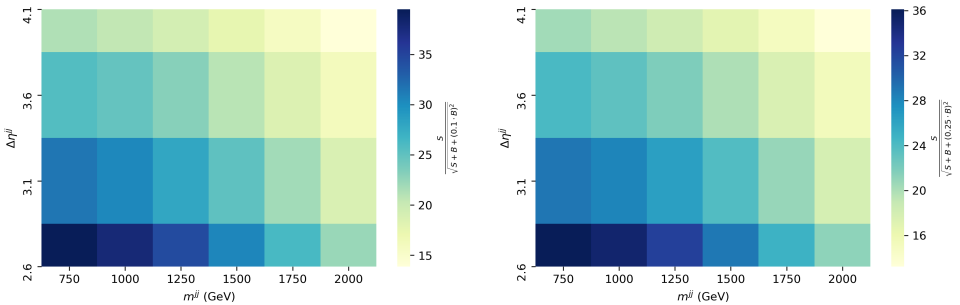

Jet Variable Selection Optimization, Again ($\Delta\eta^{jj}$, m^{jj})

Process

- Returned to the jet variables to study significance in $\Delta\eta^{jj}$, m^{jj} phase space for each of our four pairs of $m^{\gamma\gamma}$, p_T^{γ} cuts
- Performed smaller gridsearch, with selection pairs $|\Delta\eta^{jj}| > \eta_1$, $m^{jj} > m_1^j$ in the following values (m_1^j also in GeV)

  $(\eta_1, m_1^j) \in \{2.6, 3.1, 3.6, 4.1\} \times \{750, 1000, 1250, 1500, 1750, 2000\}$
- Computed significance just once on each of these $4 \cdot 6 = 24$ scenarios, using the systematic uncertainty coefficient which led to the choice of that particular $m^{\gamma\gamma}$, p_T^{γ} selection; plots are ordered as follows

  $(m_0^{\gamma}, \gamma_0) = (400, 250), (m_0^{\gamma}, \gamma_0) = (500, 300), (m_0^{\gamma}, \gamma_0) = (350, 250), (m_0^{\gamma}, \gamma_0) = (400, 350)$

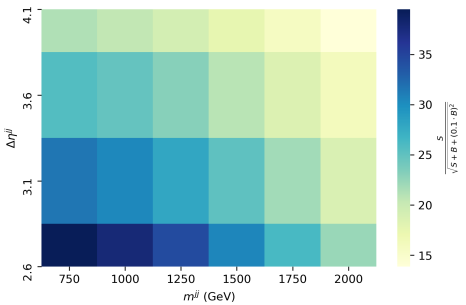

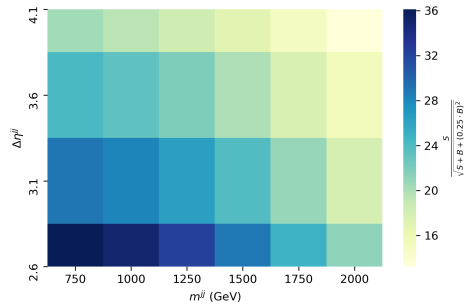

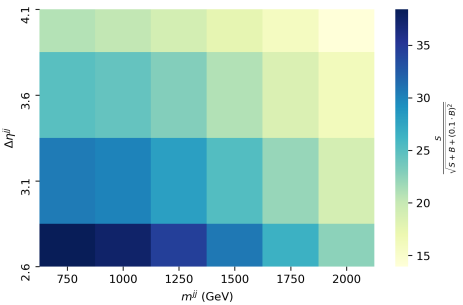

Jet Variable Selection Optimization, Again ($\Delta\eta^{jj}$, m^{jj})

Process

- Returned to the jet variables to study significance in $\Delta\eta^{jj}$, m^{jj} phase space for each of our four pairs of $m^{\gamma\gamma}$, p_T^{γ} cuts
- Performed smaller gridsearch, with selection pairs $|\Delta\eta^{jj}| > \eta_1$, $m^{jj} > m_1^j$ in the following values (m_1^j also in GeV)

  $(\eta_1, m_1^j) \in \{2.6, 3.1, 3.6, 4.1\} \times \{750, 1000, 1250, 1500, 1750, 2000\}$
- Computed significance just once on each of these $4 \cdot 6 = 24$ scenarios, using the systematic uncertainty coefficient which led to the choice of that particular $m^{\gamma\gamma}$, p_T^{γ} selection; plots are ordered as follows

  $(m_0^{\gamma}, \gamma_0) = (400, 250), (m_0^{\gamma}, \gamma_0) = (500, 300), (m_0^{\gamma}, \gamma_0) = (350, 250), (m_0^{\gamma}, \gamma_0) = (400, 350)$

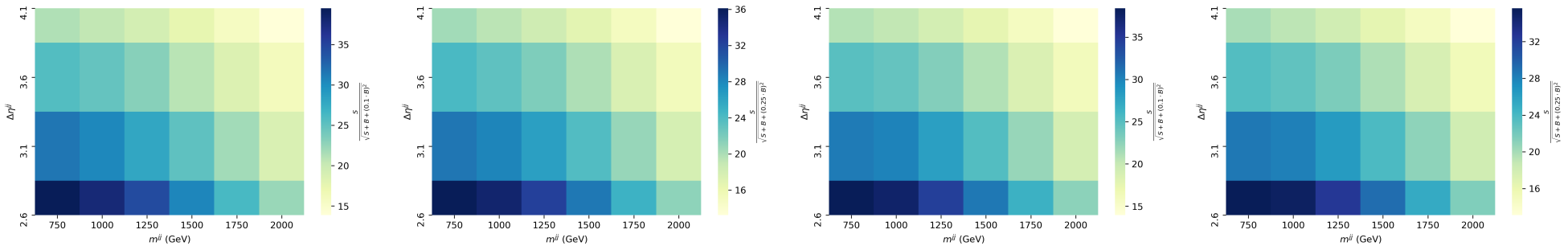

Jet Variable Selection Optimization, Again ($\Delta\eta^{jj}$, m^{jj})

Process

- Returned to the jet variables to study significance in $\Delta\eta^{jj}$, m^{jj} phase space for each of our four pairs of $m^{\gamma\gamma}$, p_T^{γ} cuts
- Performed smaller gridsearch, with selection pairs $|\Delta\eta^{jj}| > \eta_1$, $m^{jj} > m_1^j$ in the following values (m_1^j also in GeV)

  $(\eta_1, m_1^j) \in \{2.6, 3.1, 3.6, 4.1\} \times \{750, 1000, 1250, 1500, 1750, 2000\}$
- Computed significance just once on each of these $4 \cdot 6 = 24$ scenarios, using the systematic uncertainty coefficient which led to the choice of that particular $m^{\gamma\gamma}$, p_T^{γ} selection; plots are ordered as follows

  $(m_0^{\gamma}, \gamma_0) = (400, 250), (m_0^{\gamma}, \gamma_0) = (500, 300), (m_0^{\gamma}, \gamma_0) = (350, 250), (m_0^{\gamma}, \gamma_0) = (400, 350)$

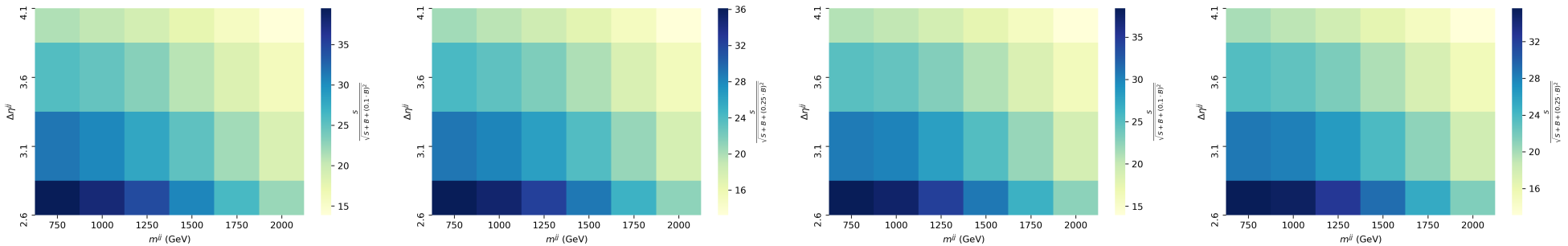

Conclusions

Jet Variable Selection Optimization, Again ($\Delta\eta^{jj}$, m^{jj})

Process

- Returned to the jet variables to study significance in $\Delta\eta^{jj}$, m^{jj} phase space for each of our four pairs of $m^{\gamma\gamma}$, p_T^{γ} cuts
- Performed smaller gridsearch, with selection pairs $|\Delta\eta^{jj}| > \eta_1$, $m^{jj} > m_1^j$ in the following values (m_1^j also in GeV)

  $(\eta_1, m_1^j) \in \{2.6, 3.1, 3.6, 4.1\} \times \{750, 1000, 1250, 1500, 1750, 2000\}$
- Computed significance just once on each of these $4 \cdot 6 = 24$ scenarios, using the systematic uncertainty coefficient which led to the choice of that particular $m^{\gamma\gamma}$, p_T^{γ} selection; plots are ordered as follows

  $(m_0^{\gamma}, \gamma_0) = (400, 250), (m_0^{\gamma}, \gamma_0) = (500, 300), (m_0^{\gamma}, \gamma_0) = (350, 250), (m_0^{\gamma}, \gamma_0) = (400, 350)$

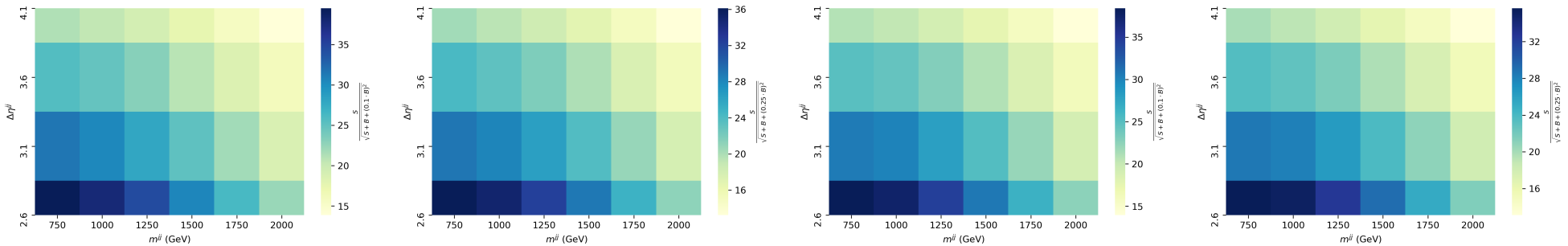

Conclusions

- Our four scenarios exhibit an approximately uniform shape, with a maximum near $(\eta_1, m_1^j) = (2.6, 750)$

Jet Variable Selection Optimization, Again ($\Delta\eta^{jj}$, m^{jj})

Process

- Returned to the jet variables to study significance in $\Delta\eta^{jj}$, m^{jj} phase space for each of our four pairs of $m^{\gamma\gamma}$, p_T^{γ} cuts
- Performed smaller gridsearch, with selection pairs $|\Delta\eta^{jj}| > \eta_1$, $m^{jj} > m_1^j$ in the following values (m_1^j also in GeV)

  $(\eta_1, m_1^j) \in \{2.6, 3.1, 3.6, 4.1\} \times \{750, 1000, 1250, 1500, 1750, 2000\}$
- Computed significance just once on each of these $4 \cdot 6 = 24$ scenarios, using the systematic uncertainty coefficient which led to the choice of that particular $m^{\gamma\gamma}$, p_T^{γ} selection; plots are ordered as follows

  $(m_0^{\gamma}, \gamma_0) = (400, 250), (m_0^{\gamma}, \gamma_0) = (500, 300), (m_0^{\gamma}, \gamma_0) = (350, 250), (m_0^{\gamma}, \gamma_0) = (400, 350)$

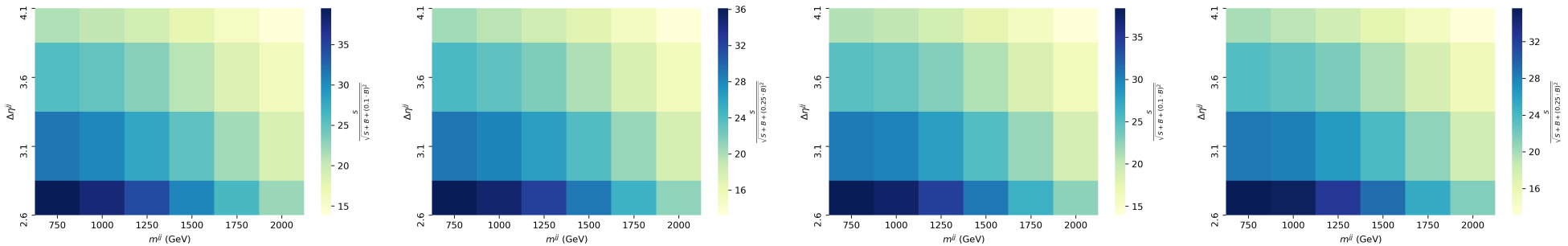

Conclusions

- Our four scenarios exhibit an approximately uniform shape, with a maximum near $(\eta_1, m_1^j) = (2.6, 750)$
  - Once again, we consider high $\Delta\eta^{jj}$ selections to be more experimentally feasible

Jet Variable Selection Optimization, Again ($\Delta\eta^{jj}$, m^{jj})

Process

- Returned to the jet variables to study significance in $\Delta\eta^{jj}$, m^{jj} phase space for each of our four pairs of $m^{\gamma\gamma}$, p_T^{γ} cuts
- Performed smaller gridsearch, with selection pairs $|\Delta\eta^{jj}| > \eta_1$, $m^{jj} > m_1^j$ in the following values (m_1^j also in GeV)

  $(\eta_1, m_1^j) \in \{2.6, 3.1, 3.6, 4.1\} \times \{750, 1000, 1250, 1500, 1750, 2000\}$
- Computed significance just once on each of these $4 \cdot 6 = 24$ scenarios, using the systematic uncertainty coefficient which led to the choice of that particular $m^{\gamma\gamma}$, p_T^{γ} selection; plots are ordered as follows

  $(m_0^{\gamma}, \gamma_0) = (400, 250), (m_0^{\gamma}, \gamma_0) = (500, 300), (m_0^{\gamma}, \gamma_0) = (350, 250), (m_0^{\gamma}, \gamma_0) = (400, 350)$

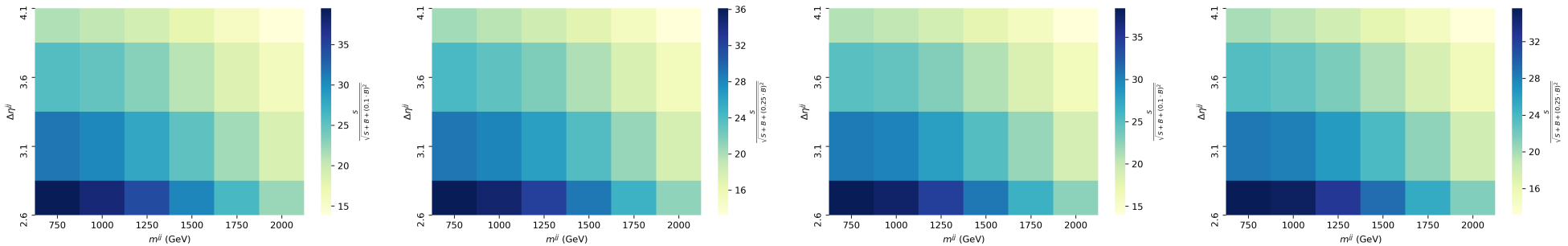

Conclusions

- Our four scenarios exhibit an approximately uniform shape, with a maximum near $(\eta_1, m_1^j) = (2.6, 750)$
  - Once again, we consider high $\Delta\eta^{jj}$ selections to be more experimentally feasible
  - We also seek to incorporate a realistically high systematic uncertainty

Jet Variable Selection Optimization, Again ($\Delta\eta^{jj}$, m^{jj})

Process

- Returned to the jet variables to study significance in $\Delta\eta^{jj}$, m^{jj} phase space for each of our four pairs of $m^{\gamma\gamma}$, p_T^{γ} cuts
- Performed smaller gridsearch, with selection pairs $|\Delta\eta^{jj}| > \eta_1$, $m^{jj} > m_1^j$ in the following values (m_1^j also in GeV)

  $(\eta_1, m_1^j) \in \{2.6, 3.1, 3.6, 4.1\} \times \{750, 1000, 1250, 1500, 1750, 2000\}$
- Computed significance just once on each of these $4 \cdot 6 = 24$ scenarios, using the systematic uncertainty coefficient which led to the choice of that particular $m^{\gamma\gamma}$, p_T^{γ} selection; plots are ordered as follows

  $(m_0^{\gamma}, \gamma_0) = (400, 250), (m_0^{\gamma}, \gamma_0) = (500, 300), (m_0^{\gamma}, \gamma_0) = (350, 250), (m_0^{\gamma}, \gamma_0) = (400, 350)$

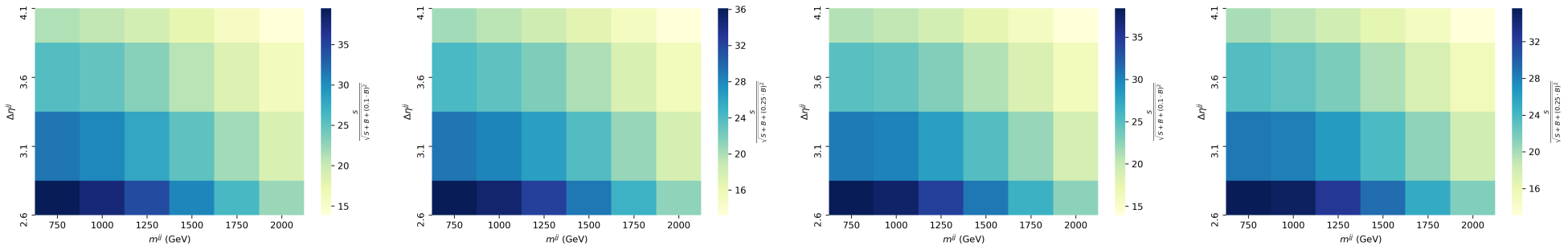

Conclusions

- Our four scenarios exhibit an approximately uniform shape, with a maximum near $(\eta_1, m_1^j) = (2.6, 750)$
  - Once again, we consider high $\Delta\eta^{jj}$ selections to be more experimentally feasible
  - We also seek to incorporate a realistically high systematic uncertainty
- These priorities motivate the following selections: $|\Delta\eta^{jj}| > 3.6$, $m^{jj} > 750$, $m^{\gamma\gamma} > 500$, $p_T^{\gamma} > 300$

Selection Significance

Selection Significance

Objective

We seek to quickly evaluate our new parameter selections.

Selection Significance

Objective

We seek to quickly evaluate our new parameter selections.

- Want to compare signal-background kinematic plots normalized to cross section between before (left) and after (center) selections are made

Selection Significance

Objective

We seek to quickly evaluate our new parameter selections.

- Want to compare signal-background kinematic plots normalized to cross section between before (left) and after (center) selections are made
- Want to examine how significance scales with luminosity for different systematic uncertainties (right)

Selection Significance

Objective

We seek to quickly evaluate our new parameter selections.

- Want to compare signal-background kinematic plots normalized to cross section between before (left) and after (center) selections are made
- Want to examine how significance scales with luminosity for different systematic uncertainties (right)

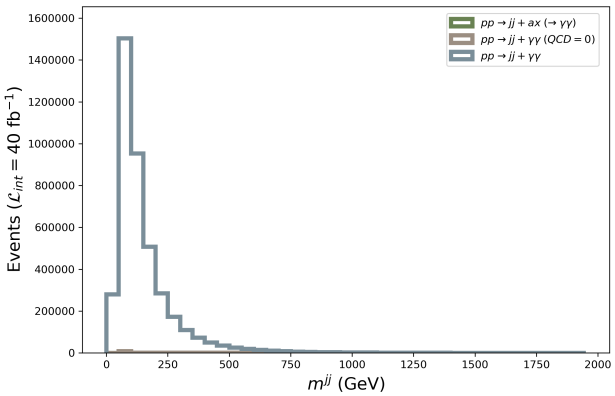

Selection Significance

Objective

We seek to quickly evaluate our new parameter selections.

- Want to compare signal-background kinematic plots normalized to cross section between before (left) and after (center) selections are made
- Want to examine how significance scales with luminosity for different systematic uncertainties (right)

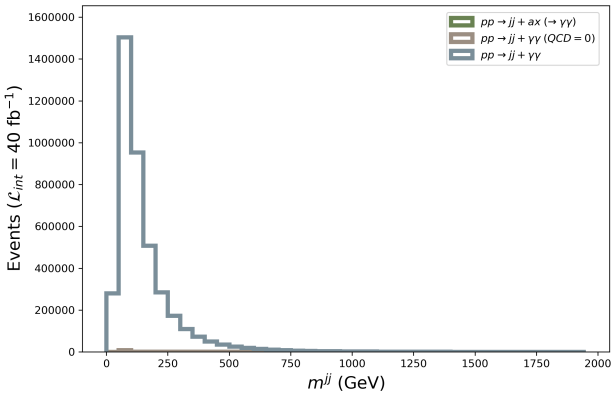

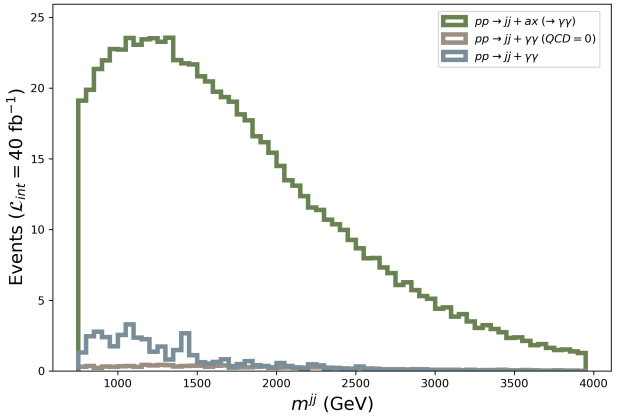

Selection Significance

Objective

We seek to quickly evaluate our new parameter selections.

- Want to compare signal-background kinematic plots normalized to cross section between before (left) and after (center) selections are made
- Want to examine how significance scales with luminosity for different systematic uncertainties (right)

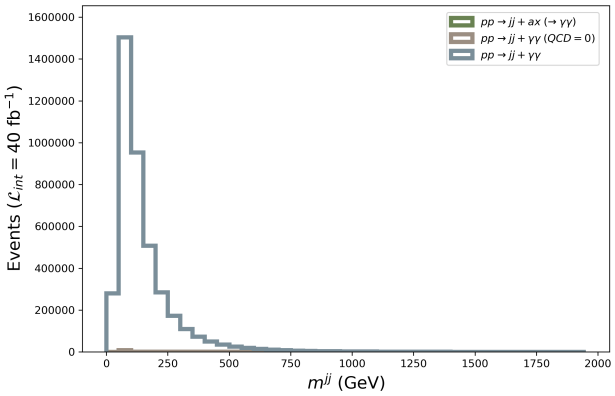

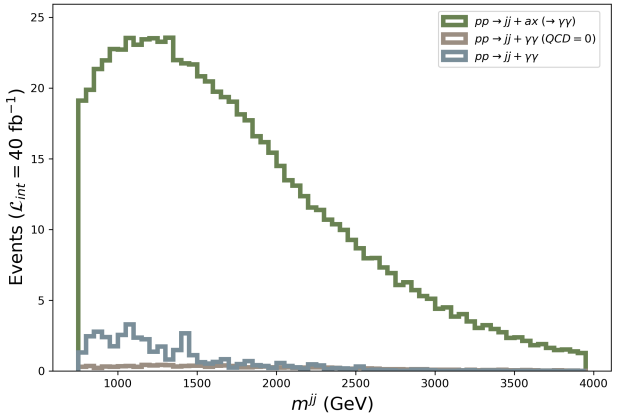

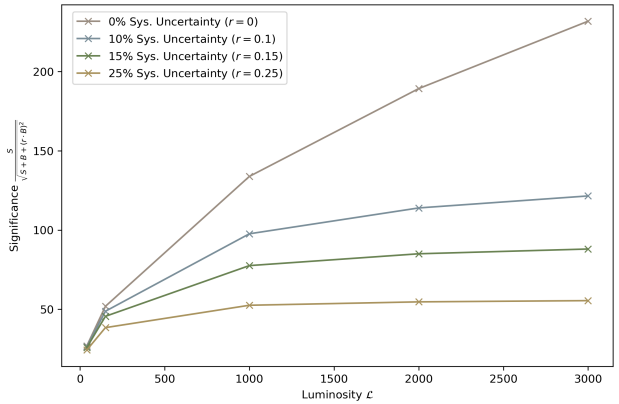

Selection Significance

Objective

We seek to quickly evaluate our new parameter selections.

- Want to compare signal-background kinematic plots normalized to cross section between before (left) and after (center) selections are made
- Want to examine how significance scales with luminosity for different systematic uncertainties (right)

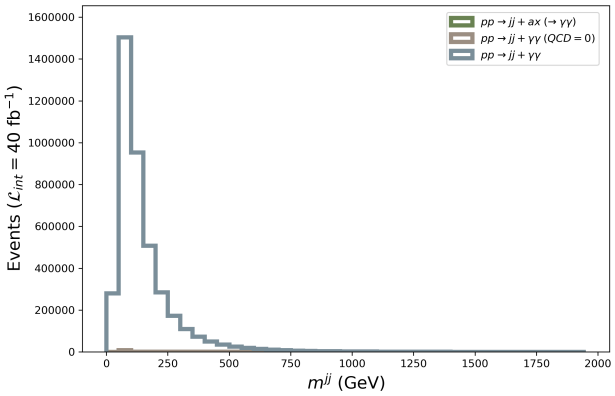

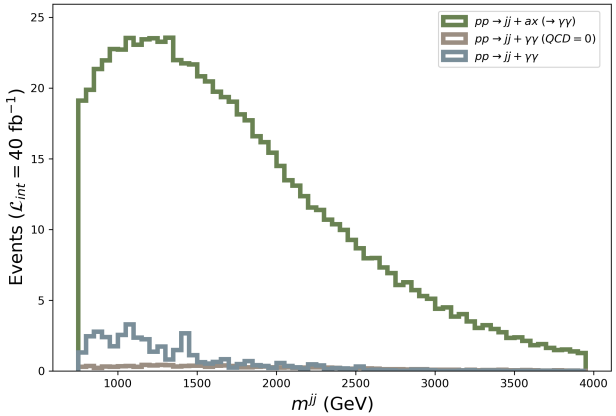

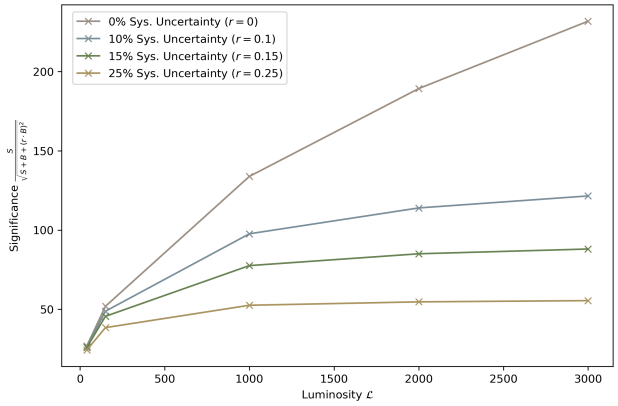

Conclusions

We've selected a region of phase space where our new physics processes dominate and discovery potential is high.

Final Thoughts

Final Thoughts

Summary

Final Thoughts

Summary

- Introduced the theory of our particular BSM interest–the axion–and the collider topology we plan to use to study it, vector boson fusion (VBF)

Final Thoughts

Summary

- Introduced the theory of our particular BSM interest–the axion–and the collider topology we plan to use to study it, vector boson fusion (VBF)
- Discussed our generation of signal events, including imposed MadGraph-level selections to increase VBF purity

Final Thoughts

Summary

- Introduced the theory of our particular BSM interest–the axion–and the collider topology we plan to use to study it, vector boson fusion (VBF)
- Discussed our generation of signal events, including imposed MadGraph-level selections to increase VBF purity
- Examined our generation of background events, including the choice of two distinct background channels and our H_T binning process

Final Thoughts

Summary

- Introduced the theory of our particular BSM interest–the axion–and the collider topology we plan to use to study it, vector boson fusion (VBF)
- Discussed our generation of signal events, including imposed MadGraph-level selections to increase VBF purity
- Examined our generation of background events, including the choice of two distinct background channels and our H_T binning process
- Analyzed kinematic variables and elaborated on our three-step selection optimization process on $\Delta\eta^{jj}$, m^{jj}, $m^{\gamma\gamma}$, p_T^j, eventually arriving at an experimentally and statistically motivated selection for each of these variable

Final Thoughts

Summary

- Introduced the theory of our particular BSM interest–the axion–and the collider topology we plan to use to study it, vector boson fusion (VBF)
- Discussed our generation of signal events, including imposed MadGraph-level selections to increase VBF purity
- Examined our generation of background events, including the choice of two distinct background channels and our H_T binning process
- Analyzed kinematic variables and elaborated on our three-step selection optimization process on $\Delta\eta^{jj}$, m^{jj}, $m^{\gamma\gamma}$, p_T^j, eventually arriving at an experimentally and statistically motivated selection for each of these variable
- Investigated signal versus background yield and the significance associated with our four final selections

Final Thoughts

Summary

- Introduced the theory of our particular BSM interest–the axion–and the collider topology we plan to use to study it, vector boson fusion (VBF)
- Discussed our generation of signal events, including imposed MadGraph-level selections to increase VBF purity
- Examined our generation of background events, including the choice of two distinct background channels and our H_T binning process
- Analyzed kinematic variables and elaborated on our three-step selection optimization process on $\Delta\eta^{jj}$, m^{jj}, $m^{\gamma\gamma}$, p_T^j, eventually arriving at an experimentally and statistically motivated selection for each of these variable
- Investigated signal versus background yield and the significance associated with our four final selections

Next Steps

Final Thoughts

Summary

- Introduced the theory of our particular BSM interest–the axion–and the collider topology we plan to use to study it, vector boson fusion (VBF)
- Discussed our generation of signal events, including imposed MadGraph-level selections to increase VBF purity
- Examined our generation of background events, including the choice of two distinct background channels and our H_T binning process
- Analyzed kinematic variables and elaborated on our three-step selection optimization process on $\Delta\eta^{jj}$, m^{jj}, $m^{\gamma\gamma}$, p_T^j, eventually arriving at an experimentally and statistically motivated selection for each of these variable
- Investigated signal versus background yield and the significance associated with our four final selections

Next Steps

- Resolve technical issues (potentially relating to `ax > a a` decay) and study how our findings vary with axions of different masses

Final Thoughts

Summary

- Introduced the theory of our particular BSM interest–the axion–and the collider topology we plan to use to study it, vector boson fusion (VBF)
- Discussed our generation of signal events, including imposed MadGraph-level selections to increase VBF purity
- Examined our generation of background events, including the choice of two distinct background channels and our H_T binning process
- Analyzed kinematic variables and elaborated on our three-step selection optimization process on $\Delta\eta^{jj}$, m^{jj}, $m^{\gamma\gamma}$, p_T^j, eventually arriving at an experimentally and statistically motivated selection for each of these variable
- Investigated signal versus background yield and the significance associated with our four final selections

Next Steps

- Resolve technical issues (potentially relating to `ax > a a` decay) and study how our findings vary with axions of different masses
- Investigate why virtual axion processes dominate

Final Thoughts

Summary

- Introduced the theory of our particular BSM interest–the axion–and the collider topology we plan to use to study it, vector boson fusion (VBF)
- Discussed our generation of signal events, including imposed MadGraph-level selections to increase VBF purity
- Examined our generation of background events, including the choice of two distinct background channels and our H_T binning process
- Analyzed kinematic variables and elaborated on our three-step selection optimization process on $\Delta\eta^{jj}$, m^{jj}, $m^{\gamma\gamma}$, p_T^j, eventually arriving at an experimentally and statistically motivated selection for each of these variable
- Investigated signal versus background yield and the significance associated with our four final selections

Next Steps

- Resolve technical issues (potentially relating to `ax > a a` decay) and study how our findings vary with axions of different masses
- Investigate why virtual axion processes dominate
- Begin formalizing our results and writing a paper